

Accepted Manuscript

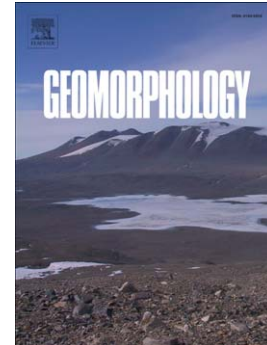
Probabilistic rainfall thresholds for triggering debris flows in a human-modified landscape

Roberto Giannecchini, Yuri Galanti, Giacomo D'Amato Avanzi, Michele Barsanti

PII: S0169-555X(15)30231-2
DOI: doi: [10.1016/j.geomorph.2015.12.012](https://doi.org/10.1016/j.geomorph.2015.12.012)
Reference: GEOMOR 5465

To appear in: *Geomorphology*

Received date: 24 April 2015
Revised date: 15 December 2015
Accepted date: 17 December 2015



Please cite this article as: Giannecchini, Roberto, Galanti, Yuri, D'Amato Avanzi, Giacomo, Barsanti, Michele, Probabilistic rainfall thresholds for triggering debris flows in a human-modified landscape, *Geomorphology* (2015), doi: [10.1016/j.geomorph.2015.12.012](https://doi.org/10.1016/j.geomorph.2015.12.012)

This is a PDF file of an unedited manuscript that has been accepted for publication. As a service to our customers we are providing this early version of the manuscript. The manuscript will undergo copyediting, typesetting, and review of the resulting proof before it is published in its final form. Please note that during the production process errors may be discovered which could affect the content, and all legal disclaimers that apply to the journal pertain.

Probabilistic rainfall thresholds for triggering debris flows in a human-modified landscape

Roberto Giannecchini^a, Yuri Galanti^{a,*}, Giacomo D'Amato Avanzi^a, Michele Barsanti^b

^a Department of Earth Sciences, University of Pisa, Via S. Maria 53, 56126, Pisa, Italy

^b Department of Civil and Industrial Engineering, University of Pisa, Largo Lucio Lazzarino 2, 56122, Pisa, Italy

* Corresponding author: Yuri Galanti, galanti@dst.unipi.it, phone: +39 050 2215700, fax: +39 050 2215800

Abstract

In the Carrara Marble Basin (CMB; Apuan Alps, Italy) quarrying has accumulated widespread and thick quarry waste, lying on steep slopes and invading valley bottoms. The Apuan Alps are one of the rainiest areas in Italy and rainstorms often cause landslides and debris flows. The stability conditions of quarry waste are difficult to assess, owing to its textural, geotechnical and hydrogeological variability. Therefore, empirical rainfall thresholds may be effective in forecasting the possible occurrence of debris flows in the CMB. Three types of thresholds were defined for three rain gauges of the CMB and for the whole area: rainfall intensity–rainfall duration (*ID*), cumulated event rainfall–rainfall duration (*ED*), and cumulated event rainfall normalized by the mean annual precipitation–rainfall intensity ($E_{MAP}I$).

The rainfall events recorded from 1950 to 2005 was analyzed and compared with the occurrence of debris flows involving the quarry waste. They were classified in events that triggered one or more debris flows and events that did not trigger debris flows. This dataset was fitted using the logistic regression method that allows us to define a set of thresholds, corresponding to different probabilities of failure (from 10% to 90%) and therefore to different warning levels. The performance of the logistic regression in defining probabilistic thresholds was evaluated by means

of contingency tables, skill scores and receiver operating characteristic (ROC) analysis. These analyses indicate that the predictive capability of the three types of threshold is acceptable for each rain gauge and for the whole CMB. The best compromise between the number of correct debris flow predictions and the number of wrong predictions is obtained for the 40% probability thresholds. The results obtained can be tested in an experimental debris flows forecasting system based on rainfall thresholds, and could have implications for the debris flow hazard and risk assessment in the CMB.

Keywords: Probabilistic rainfall threshold; Logistic regression; Debris flow; Human-modified landscape; Tuscany; ROC analysis

1. Introduction

The famous marble and a spectacular mountain landscape close to the Versilia coastline make the Apuan Alps (Tuscany, Italy) well-known in the world. Here the marble excavation is intense and quarrying areas and quarry wastes, named *ravaneti*, can dominate the landscape. In the Carrara Marble Basin (CMB; Figs. 1 and 2) the quarry density is among the highest in the world with at least 7 quarries km^{-2} , whilst the Apuan and the Italian averages are 0.33 and 0.03 quarries km^{-2} , respectively (Cortopassi et al., 2008). Marble quarrying and working are sources of income and tourist attraction and remains of ancient quarries, excavation techniques and buildings are examples of industrial archeology and geosites (D'Amato Avanzi and Verani, 2000). A long-lasting quarrying activity can cause environmental and hydrogeological problems because waste materials are commonly discharged onto the slopes, without stabilization. At present they cover wide areas and often reach and occupy the valley bottoms (Figs. 1 and 2).

The Apuan Alps are among the rainiest areas in Italy and frequently hit by heavy rainstorms, which often induce floods and landslides, sometimes causing damage and casualties (Giannecchini and D'Amato Avanzi, 2012). Mass movements and especially debris flows often involve these waste materials (Cortopassi et al., 2008). In this context, hazard assessment and early warning systems can be helpful in protecting population, workers and factories and reducing the risk. However, a lot of information is needed to model the processes leading to instability and to predict the time of failure. Various authors assert that the empirical rainfall thresholds can be used in a landslide early warning system to forecast the possible occurrence of rainfall-induced landslides (e.g., Chleborad et al., 2008; Baum and Godt, 2010; Rossi et al., 2012; Vennari et al., 2014; Calvello et al., 2015; Gariano et al., 2015; Rosi et al., 2015; Segoni et al., 2015). Hence, a black box approach can help us to overcome some difficulties in determining the rainfall thresholds to be applied in warning and civil protection activities against quarry waste instability. Historical data on debris flows and related damage can allow us to define the rainfall thresholds for the CMB, in terms of duration, cumulated event rainfall, intensity, and mean annual precipitation.

2. Study area

This paper focuses on the well-known CMB, where Michelangelo Buonarroti chose the marble for his masterpieces and a lot of quarries are working. The CMB is among the most famous and precious quarrying sites in the world. It is subdivided into the four Colonnata, Miseglia, Torano and Pescina-Boccanaglia sub-basins (Fig. 2).

The Carrara marble consists of Hettangian limestone, metamorphosed to greenschist facies during Upper Oligocene–Upper Miocene. It is part of the Apuan Alps Metamorphic Complex (Paleozoic–Upper Oligocene), the main tectonic structure of the Apuan Alps (Conti et al., 2004). The Carrara marble is a high quality, white or blue-grey ornamental stone, mostly used in sculpture and building decoration. Its beauty and many famous masterpieces make this marble very appreciated and renowned in the world. The marble exploitation has been documented since Roman times, with evidence of pre-Roman activity (Bruschi et al., 2004). In time, quarrying has more and more developed, because of increased demand and new developing markets; consequently, the number of quarries has greatly increased and the quarry waste has covered more and more vast areas.

A high frequency of intense rainfalls characterizes the Apuan area (Giannecchini and D'Amato Avanzi, 2012): because of shape, altitude (almost 2,000 m a.s.l.) and location close to the sea, the Apuan Alps intercept the Atlantic and Mediterranean humid air masses, forcing their lifting, adiabatic cooling and condensation in rain. Therefore, the mean annual precipitation (*MAP*) is higher than 3,000 mm (Fig. 3), exceeding 4,000 mm in the rainiest years.

In the Apuan area very intense rainstorms can trigger shallow landslides and debris flows, which threaten the population and may cause great problems (Table 1; D'Amato Avanzi et al., 2004; Giannecchini, 2006; Giannecchini and D'Amato Avanzi, 2012). For example, on 19 June 1996, 325 mm in 4 h and 158 mm in 1 h; and on 23 September 2003, 160 mm in 2 h and 46 mm in 15 min. The town of Carrara (about 70,000 citizens) is located along the Carrione Torrent, just downstream of the CMB (Fig. 2). The 23 September 2003 rainstorm caused flooding, debris flows, one death and severe damage to buildings, roads, quarries and factories, and quarrying was interrupted (Figs.

4 and 5). Less intense prolonged rainfalls are sometimes sufficient to induce failures in the Apuan area. In November 2000, shallow landslides were triggered by the rainfall of 160 mm in 13 h (maximum intensity of 30 mm h^{-1}), preceded by a high antecedent rainfall amount – almost 600 mm within one month (Giannecchini, 2006).

The landslides triggered by the Apuan rainstorms are typically those activated by very intense rainfall on steep slopes (Cruden and Varnes, 1996; Hungr et al., 2001, 2014). They consist of rapid shallow landslides and debris flows, with a width/length ratio typically less than one, usually mobilizing the soil covering the bedrock. In spite of the small volume involved, shallow landslides and debris flows are extremely destructive, because of their high speed and concentration. The materials involved in failures (earth, debris, blocks and trees) usually flow into the riverbeds, causing hyperconcentrated flows and debris floods.

As previously highlighted, in the CMB, human activity has radically changed the natural environment, and the geomorphological features are very different from the rest of the Apuan area. A huge amount of discharged material is available and the debris flow is an usual type of movement. This demands that the rainfall thresholds for triggering debris flows are established, in order to prevent and control the risk conditions.

3. Quarry waste features and instability problems

The quarry waste is the residual material resulting from marble excavation and is formed of angular rock fragments, variable in size and mixed with sand and other materials. It has been discharged downslope of quarrying areas. An active quarry waste is frequently loaded with new material; shape and thickness frequently change, and instability is frequent. When discharge stops, a quarry waste becomes inactive and gradually tends to be stabilized. Old or ancient wastes dating back to tens of years or centuries ago are generally more stable, due to the bigger size of clasts with respect to recent wastes, and to the stabilizing effect of natural compaction and cementation.

The evolution of quarrying techniques has led to the modification of the grain size, composition and physical-mechanical and hydrogeological properties of the quarry waste (Baroni et al., 2003; Cortopassi et al., 2008). Old and ancient quarry dumps are well sorted and coarser, and exhibit greater uniformity, while recent or active dumps are poorly sorted and include a greater amount of finer materials and sawing residue, named *marmettola* (a muddy mix of cooling water and fine, carbonate clay-rich dust). Recent exploitation and on-site sieving of coarser materials for industrial uses (calcium carbonate, filling, etc.) induce a relative increase in finer materials within the quarry waste. Then, the texture is complex and highly variable, with boulders, blocks, small fragments and finer materials (less than 2 mm). Clast- and matrix-supported levels can be present in the same deposit (Fig. 5). Finally, the older quarry waste is more permeable than the recent one, where levels of semi-permeable or impermeable *marmettola* can favor saturation and pore pressure build-up, leading to instability.

Even if the new technologies have improved efficiency in quarrying and reduced the production of waste, around 50% of the extracted material still results in waste. In the year 2000, the CMB included 167 quarries (90 were active), with a total amount of quarry waste assessed at more than 80,000,000 tons (Cortopassi et al., 2008, and references therein). At present, the waste material covers about 4–5 km² of the CMB (approximately 50% of the whole basin area). Thickness and surface of quarry waste are extremely variable in space and time: for example, surface and thickness of a large quarry waste in the Torano basin greatly increased and almost doubled, mainly in the last 20–30 years (Cortopassi et al., 2008). Bedrock morphology and waste thickness are also mostly unknown, while the active quarry dumps can quickly change shape and profile for accumulation, excavation or mass movements.

Instability of quarry waste is consequently a present issue, which has also historical roots, linked to the above-mentioned evolution of quarrying techniques. Continuous discharge and accumulation of material, excavation, slope cutting or road construction leads to overload the waste and/or to exceed its friction angle, causing slope instability. However, heavy rainfall, rainstorms and stream erosion

are probably the most important triggers of debris flows involving quarry waste and threatening population, villages and infrastructures.

A debris flow usually starts as a planar slide, which quickly disaggregates and becomes a very or extremely rapid debris flow, travelling in an erosive channel (Baroni et al., 2000, 2010). A contraction mechanism is probably responsible for a reduction of the consistency, and consequently of the collapsing and flowing of the saturated material (Ellen and Fleming, 1987; Cruden and Varnes, 1996; Iverson et al., 1997). In the CMB the channelized debris flows prevail, while open-slope debris flows are a minority; travel distance vary between some tens and hundreds of meters. In steep riverbeds, saturation of the waste and free water flowing can directly mobilize the deposit, triggering channelized debris flows. The latter can travel long distances downstream and reach populated areas. These particular mass movements can be classified either as complex, rapid to extremely rapid debris slide-debris flows (Cruden and Varnes, 1996), or as extremely rapid, saturated debris flows following established channels over a large part of their path (Hungri et al., 2001).

This high-risk state needs to be controlled and prevented by means of good practices in the quarrying sector and environmental management. In this context, hazard assessment and early warning systems can be crucial in protecting the population, workers and factories and reducing the risk. However, a lot of information is needed to know the processes leading to instability, apply physically based models and predict the time of failure. A complete characterization of quarry waste would be very time and money consuming. Therefore, at present the physical and mechanical properties of quarry waste are virtually unknown and information is sporadic and incomplete.

The strength of quarry waste usually depends on the friction angle, unless abundant finer materials or cementation provide it with cohesion. The few available data come from literature, back-analysis of failed material or design of remedial works (Marachi et al., 1972; Barton and Kjaernsli, 1981; Panei et al., 2000; Barton, 2008). Due to the above-mentioned scarcity of data, the stability analyses

of the quarry waste in the CMB are rare and at present do not allow a zonation of the stability condition of the quarry waste.

4. Rainfall thresholds: state of art

In the scientific literature, two approaches have been proposed in evaluating the relationship between rainfall and landslide occurrence. The first one is based on physical threshold models (Montgomery and Dietrich, 1994; Wu and Sidle, 1995; Iverson, 2000; Baum et al., 2010; Bartelletti et al., 2015), whereas the second approach relies on the definition of empirical thresholds (Caine, 1980; Aleotti, 2004; Giannecchini, 2006; Guzzetti et al., 2007, 2008; Cannon et al., 2008, 2011; Dahal and Hasegawa, 2008, Brunetti et al., 2010; Saito et al., 2010; Giannecchini et al., 2012; Martelloni et al., 2012; Peruccacci et al., 2012; Tien Bui et al., 2013; Segoni et al., 2014a,b; Vennari et al., 2014; Zêzere et al., 2015; Melillo et al., 2015; Gariano et al., 2015). Physical threshold models require detailed spatial information on the hydrological, lithological, morphological and geotechnical characteristics of the materials involved in landsliding, and therefore may be applied only in small areas (D'Amato Avanzi et al., 2013b).

The empirical approach can be obtained in relation to the geographical extent over which the rainfall threshold is defined (i.e., global, national, regional or local), and to the type of rainfall information used to determine it (Guzzetti et al., 2007, 2008). Rainfall duration (D), cumulated event rainfall (E), intensity (I), and antecedent rainfall (A_D) are the typically investigated variables. Landslide initiation is frequently related to I and D (Caine, 1980; Aleotti, 2004; Giannecchini, 2006; Guzzetti et al., 2007, 2008; Cannon et al., 2008; Dahal and Hasegawa, 2008; Giannecchini et al., 2012).

Antecedent rainfall, geological and climatic context play important roles in triggering landslides, but the rate of water infiltration and its movement below the surface are the key aspects of landslide initiation and are considered in physically based, process driven methods (Caine, 1980; Iverson, 2000; Giannecchini et al., 2007; D'Amato Avanzi et al., 2009; Zizioli et al., 2013; Ma et al., 2014;

Rianna et al., 2014; Bordoni et al., 2015). The empirical approach avoids the quantification of the parameters required by the physically-based models and allows us to investigate wider areas.

As highlighted by Cannon et al. (2008), an empirical rainfall threshold is typically obtained by one of the three following approaches. The first one is the determination of the lower limit of rainfall conditions (e.g., rainfall duration and intensity) above which shallow landslides occurred (e.g., Caine, 1980; Godt et al., 2006; Cannon et al., 2008). The thresholds obtained by this limit represent the most conservative rainfall conditions (e.g., lower rainfall intensity) for the shallow landslides initiation (Staley et al., 2013). The second approach defines the threshold at the upper limit of rainfall conditions that did not induce failures (e.g., Cannon and Ellen, 1988; Cannon et al., 2008). These thresholds represent a less conservative estimation of triggering conditions (e.g., higher rainfall intensity), even if shallow landslides often initiate at lower rainfall intensity (Cannon et al., 2008). The third approach defines the rainfall thresholds separating rainfall events that triggered shallow landslides from events that did not (Wieczorek and Sarmiento, 1988; Larsen and Simon, 1993; Terlien, 1998; Jakob and Weatherly, 2003; Giannecchini, 2006, 2012, 2014; Frattini et al., 2009; Staley et al., 2013). This separation process is however difficult; some authors (Chang et al., 2008; Frattini et al., 2009; Giannecchini et al., 2014) used the logistic regression to define the probability that a rainfall of a given duration and intensity triggers a landslide. This method was applied in this study.

5. Rainfall events in the study area

All the main rainfall events occurred in the CMB from 1950 to 2005 were identified and analyzed. Unfortunately, no rain gauge of the study area has a continuous record of hourly rainfall for this period. Therefore, three rain gauges were considered, located at Fossacava (624 m a.s.l., 1950–1964), Rif. Belvedere (1,276 m a.s.l., 1968–1990) and Carrara (55 m a.s.l., 1990–2005) (see Fig. 2 for their locations). In this way, the 1950–2005 interval was almost fully covered. The historical series of rainfall data of the Fossacava and Rif. Belvedere rain gauges are quite short, while the

Carrara rain gauge has a long historical series. The latter was placed in 1929, but hourly rainfall records are available only after 1990. The three rain gauges are quite close (7 km from Carrara to Rif. Belvedere and Fossacava and 5 km from Rif. Belvedere to Fossacava; Fig. 2), but their altitudes are different; consequently their *MAP* value is also different, rising with the altitude: 1,376 mm at Carrara, 1,540 mm at Fossacava, and 1,664 mm at Rif. Belvedere. Rain gauges placed at different location and altitude can record different rainfall values for the same event. The *MAP* normalization of the rainfall data can decrease the influence of the simultaneous use of two or more rain gauges in the rainfall threshold definition, and allows us to analyze and compare the rainfall thresholds at different elevations. The frequency of the extreme rainfall events estimated by the rain gauges can also influence the rainfall thresholds. However, the return periods of extreme rainfall events of short duration (1, 3, 6, 12 and 24 h), for the whole CMB are similar (Caporali et al., 2014a; Centro Funzionale Regione Toscana, 2015). Considering the short distance among the rain gauges and the homogeneous frequency of extreme rainfall events in the study area, the simultaneous use of three rain gauges in determining the CMB rainfall thresholds may be acceptable.

All the rain gauges have been equipped with pluviographs for all the recording period. The pluviographs require a manual extraction of the hourly rainfall data, which is a hard and time consuming activity. We assume that the rainfall events less intense than 1 mm h^{-1} (irrespective of their duration) have little influence on the computation of rainfall thresholds by logistic regression, and can be neglected to save time and resources. Therefore, 191 significant rainfall events were found and analyzed in the 1950–2005 period. Events with short duration (2–3 h) and high intensity ($20\text{--}30 \text{ mm h}^{-1}$), or those with long duration (100–120 h) and low intensity ($1\text{--}2 \text{ mm h}^{-1}$), and intermediate events were considered. For each event the following data were collected: (i) cumulated event rainfall (E , in mm), (ii) rainfall duration (D , in h), and (iii) rainfall intensity (I , in mm h^{-1}). Afterwards, a detailed archive research was performed on the consequences of the selected events on quarry wastes stability. Usually in areas characterized by intense human activities, scars and deposits of debris flows and shallow landslides are rapidly restored, whilst in a

natural environment vegetation can hide them, without leaving any significant geomorphological evidence (Giannecchini and D'Amato Avanzi, 2012). In this context, the landslides of quarry waste should be detected within few days after their initiation by field surveys. Otherwise, they can be mapped by analysis of aerial photographs (if available). In the latter instance, it is difficult or even impossible to determine the time of landslide occurrence. If landslide inventory maps are not available or the time of occurrence of the mapped landslides is unknown, an archive research can be a valid, and maybe the only means to identify the size of the consequences of past events.

The archive research was based on the analysis and verification of data coming from different sources: (i) municipal administrations, (ii) the Civil Protection Service of the Massa-Carrara Province, (iii) fire brigades, (iv) technical and scientific reports, (v) newspapers, (vi), and population and workers. Most of information came from the local newspapers.

Based on their consequences, the 191 events investigated were subdivided into two groups: (i) events that triggered one or more debris flows (DF) and (ii) events that did not trigger debris flows (NDF). Table 2 shows number and percentage of DFs and NDFs for each rain gauge and for all the rain gauges of the CMB.

Debris flows frequently occur before the end of a rainfall event. The rainfalls recorded after the time of occurrence were not used in selecting the rainfall events responsible for debris flows; consequently, the rainfall variables of DF events were computed between the start of the event and the time of debris flow occurrence. All the DF events triggered debris flows in the quarry waste and sometimes shallow landslides on natural slopes. However, there is often little information on the consequences of the past rainstorms.

Since the three analyzed rain gauges have different operating periods, the rainfall thresholds were defined for each rain gauge and for the whole study area (CMB), using the rainfall data recorded in all the rain gauges in the 1950–2005 period.

6. Definition of rainfall thresholds

In this work, three types of rainfall thresholds were defined: (i) rainfall intensity–rainfall duration (ID), (ii) cumulated event rainfall–rainfall duration (ED), and (iii) cumulated event rainfall normalized by MAP –rainfall intensity ($E_{MAP}I$). They were chosen for the following reasons:

(i) In the scientific literature, the ID type rainfall thresholds prevail (Guzzetti et al., 2007, 2008, and references therein) and are available for comparisons.

(ii) Considering the rainfall amount needed to trigger a debris flow, ID and ED thresholds are equivalent. Indeed, the mean rainfall intensity I is obtained by dividing the cumulated rainfall E by the duration D of the event, $I = E/D$ (Guzzetti et al., 2007; Perruccacci et al., 2012). As suggested by Perruccacci et al. (2012), in a landslide forecasting system the use of ED thresholds is handier than that of ID thresholds. During a rainfall event, the use of ED does not imply the conversion of the cumulated rainfall E (measured at rain gauges or forecasted by numerical meteorological models) in the corresponding mean intensity rainfall I , without consuming time and resources.

(iii) Various authors assert that each area is in equilibrium with its rainfall conditions (Guidicini and Iwasa, 1977; Cannon, 1988; Aleotti, 2004; Giannecchini, 2006; Giannecchini et al., 2012). Therefore, in order to normalize the rainfall data, they are commonly compared with MAP . The use of E_{MAP} facilitates the comparison between rainfall thresholds obtained for regions with different rainfall conditions.

6.1. Outline of logistic regression

The rainfall thresholds were determined using statistical techniques to separate rainfall events that induced DFs from NDFs. As explained above, the events with $I < 1 \text{ mm h}^{-1}$, independently of their duration, were not considered in the analysis. A partial overlapping of the DF and NDF events makes it difficult, and probably inappropriate, to define a single threshold curve. Thus, it is better to define the probability (p) that a couple of rainfall variables can trigger a debris flow. This probability of occurrence can be estimated using logistic regression.

Logistic regression is useful when the dependent variable is categorical (e.g., presence/absence) and the explanatory variables are categorical, numeric or both (Menard, 2001; Agresti, 2010). The logit model from a logistic regression has the following form:

$$\text{logit}(p) = \beta_0 + \beta_1 x_1 + \beta_2 x_2 + \dots + \beta_n x_n \quad (1)$$

where $\text{logit}(p)$ is the dependent variable, x_i is the i -th explanatory variable, β_i the regression coefficient associated with the explanatory variable x_i , with $i = 1 \dots n$.

$\text{logit}(p)$ is the natural logarithm of the odds:

$$\text{logit}(p) = \ln(p/(1-p)) \quad (2)$$

where p is the probability of occurrence of DFs and $p/(1-p)$ is the odds. Converting $\text{logit}(p)$ to the probability p , Eq. (2) can be rewritten as:

$$p = \frac{1}{1 + \exp[-(\beta_0 + \beta_1 x_1 + \beta_2 x_2 + \dots + \beta_n x_n)]} \quad (3)$$

A posteriori values of probability $p = 1$ and $p = 0$ were assigned to DF and NDF events, respectively. The best-fit values of β_i were determined using a maximum-likelihood fitting technique in R software (generalized linear model – GLM, command of the built-in package STATS; R Core Team, 2014). For each dataset, several couples of variables ($n = 2$) were chosen: $\log_{10}D - \log_{10}I$, $\log_{10}D - \log_{10}E$ and $\log_{10}I - \log_{10}E_{MAP}$.

For simplicity, it is possible to define $\tilde{I} = \log_{10} I$ and $\tilde{D} = \log_{10} D$, obtaining:

$$p = \frac{1}{1 + \exp[-(\beta_0 + \beta_1 \tilde{D} + \beta_2 \tilde{I})]} \quad (4)$$

and consequently:

$$\tilde{I} = -\frac{\beta_1}{\beta_2} \tilde{D} - \frac{1}{\beta_2} \left[\ln \left(\frac{1-p}{p} \right) + \beta_0 \right] \quad (5)$$

The relationship between the variables of the model can be simplified, defining: $\beta'_1 = \beta_1 \log_{10}[\exp(1)]$, $\beta'_2 = \beta_2 \log_{10}[\exp(1)]$ and $\beta'_0 = \beta_0$. In this way, Eq. (5) can be written as:

$$I = \exp \left(-\frac{\beta'_0}{\beta'_2} \right) \left(\frac{1-p}{p} \right)^{-\frac{1}{\beta'_2}} D^{-\frac{\beta'_1}{\beta'_2}} \quad (6)$$

Likewise for the other couples of variables, the final equations are:

$$E = \exp \left(-\frac{\beta''_0}{\beta''_2} \right) \left(\frac{1-p}{p} \right)^{-\frac{1}{\beta''_2}} D^{-\frac{\beta''_1}{\beta''_2}} \quad (7)$$

$$E_{MAP} = \exp \left(-\frac{\beta'''_0}{\beta'''_2} \right) \left(\frac{1-p}{p} \right)^{-\frac{1}{\beta'''_2}} I^{-\frac{\beta'''_1}{\beta'''_2}} \quad (8)$$

For simplicity, Eq. (6) can be expressed in the form:

$$I = \alpha D^\gamma \quad (9)$$

where α is the intercept on the y-axis and γ is the shape parameter that defines the slope of the power law curve. α and γ are defined as:

$$\alpha = \exp \left(-\frac{\beta'_0}{\beta'_2} \right) \left(\frac{1-p}{p} \right)^{-\frac{1}{\beta'_2}} \quad (10)$$

$$\gamma = -\frac{\beta_1'}{\beta_2'} \quad (11)$$

Eqs. (7) and (8) can be written in a simplified form, similar to Eq. (9).

Being the graphs shown in the following sections in bi-logarithmic scale, the iso-probability curves are straight lines parallel to each other. For each fit (i) the maximum-likelihood estimates of the parameters, (ii) a test of significance for each variable, and (iii) some parameters for the evaluation of the goodness of fit are shown.

6.2. ROC analysis

The receiver operating characteristic (ROC) analysis is a method for assessing the performance of a classification model (Swets et al., 1988; Fawcett, 2006), and can be used to evaluate models that produce discrete predictions (two or more classes) or continuous ones (e.g., probability). Recently, the ROC analysis has been used to assess the performance of rainfall thresholds (e.g., Staley et al., 2013; Mathew et al., 2014; Gariano et al., 2015), as in this study.

Being the output of a logistic regression a continuous predictor (probability), it must be transformed in a dichotomous one using a threshold value. A binary classifier model presents four possible outcomes that can be graphically represented using a contingency table (Staley et al., 2013; Fig. 6a). For each event, the occurrence is considered to be either true or false (if either occurred or did not occur), while the model predictions are considered to be positive or negative (successful prediction or wrong prediction). Based on this classification, for each threshold type and probability of debris flow occurrence, the rainfall (DF + NDF) events were classified as follows: true positives (rainfall conditions exceed the threshold and at least a debris flow occurs; their number is referred to as *TP*), true negatives (no threshold overcoming, no debris flow; *TN*), false positives (threshold overcoming, no debris flow; *FP*), and false negatives (no threshold overcoming but at least a debris flow occurs; *FN*). In a landslide warning system, *FP* shows false alarms and *FN* shows missed alarms. Gariano

et al. (2015) observed that the use of high thresholds (high probability of debris flow occurrence), increases FN , while TP decreases. Conversely, using low thresholds (low probability of debris flow occurrence) FP increases and TN decreases.

In a deeply human-modified landscape such as the CMB, the uncertainty on the consequences of the rainfall events is a big problem for an archive research. After a rainstorm the quarrying areas are quickly restored, in order to limit the consequences for population and working activities. In this context and using the past rainfall events, several false positives can result from the lack of information on landslides occurrence (i.e., debris flows may have occurred but may not be reported). For this reason, several events may be wrongly counted in TN and FP and, consequently, the probabilistic thresholds could be slightly underestimated. Furthermore, as highlighted in Section 5, many events without debris flows (hypothetically close to the lower left corner of the threshold graphs) were not used in the logistic regression, and consequently TN was underestimated. This underestimation influences some skill scores calculated by the contingencies.

Using TP , TN , FP , and FN , the following skill scores were calculated (Fig. 6a):

- Probability of detection (POD) or true positive rate (TP_{rate}): proportion of debris flow events correctly predicted;
- Probability of false detection ($POFD$) or false positive rate (FP_{rate}): proportion of correct predictions when the event did not occur;
- Probability of false alarm ($POFA$): ratio between the number of false alarms and the total number of forecasts;
- Efficiency (Ef): ratio between the number of successful predictions and the total number of events;
- Hanssen and Kuipers (1965) skill score (HK): accuracy of prediction for the events with and without debris flows. HK represents the difference between POD and $POFD$.

As suggested by Gariano et al. (2015), the skill scores were defined based on the terminology proposed by Barnes et al. (2009). Fig. 6a shows the formula of each skill score used to evaluate the performance of the thresholds. The values of POD , $POFD$, $POFA$, and Ef range between 0 and 1; for POD and Ef the optimal value is 1, while $POFD$ and $POFA$ the optimal value is 0. HK ranges between -1 and 1 , where 1 is its optimal value.

The predicting capability of rainfall thresholds for different probability of debris flow occurrence can be tested using an ROC analysis. In an ROC space the relationship between POD and $POFD$ is plotted, obtaining the AUC (area under curve) value (Fig. 6b). The higher is the AUC value, more performing is the model; when $AUC = 0.5$ (Fig. 6b), the model has no prediction capability (the ROC curve is the diagonal of the square). In the opposite limit case ($AUC = 1$; Fig. 6b), the ROC curve corresponds to the upper side of the square and the model capability prediction is the best.

7. Results and discussion

7.1. Probabilistic rainfall thresholds for the CMB

The analysis of the rainfall data highlighted that very heavy rainstorms occurred on 5 October, 1955, 27 November 1962, 17 November 1968, 8 June 1973, 1 November 1977, 4 October 1978, 7 November 1994, 30 October 2000, 21 September 2002, and 23 September 2003. The analyzed events mainly occurred in autumn (September–November period; Fig. 7). Giannecchini (2006) found a comparable distribution for the Southern Apuan Alps, while Guzzetti (2000) and Guzzetti et al. (2005) obtained similar results on a national scale for rainfall that caused deaths or missing people. Fig. 7 shows the seasonal distribution of all the analyzed rainstorms (DF + NDF; Fig. 7a) and of those inducing debris flows (DF; Fig. 7b). The most severe rainstorms usually occurred between September and November and, secondly, in the December–February period.

For each rain gauge and for all the rain gauges (CMB), ID , ED and $E_{MAP}I$ thresholds for different probability of debris flow occurrence were defined using the logistic regression, as described in Section 6.1. Tables 3, 4 and 5 show the best-fit parameters (β_0 , β_1 and β_2) and the related p -values

(significant level) obtained for three sets of explanatory variables ($D-I$, $D-E$ and $I-E_{MAP}$) for Carrara, Fossacava, Rif. Belvedere and the CMB. A low p -value indicates that the introduction of the corresponding variable in the fitting function is significant, namely it is reasonable to assume that the parameter is significantly different from zero. When the p -value exceeds the typical value of 0.05, the associated parameter is considered not significant; this means that its introduction does not affect significantly the computed value of probability.

Using the results obtained with the GLM command of R software, equiprobability curves (probabilistic rainfall thresholds) can be drawn. Each curve corresponds to a probability of debris flow occurrence. The equations shown in Table 6 and Figs. 8, 9 and 10 allow us to define the ID , ED and $E_{MAP}I$ thresholds (at a chosen value of p) for Carrara, Fossacava, Rif. Belvedere and the CMB. By varying the value of p in the range from 0 to 1 in the equations; it is possible to get the rainfall threshold for each desired probability of debris flow occurrence. Figs. 8, 9 and 10 show the probabilistic ID , ED and $E_{MAP}I$ thresholds for 10%, 30%, 50%, 70%, and 90% probability of debris flow occurrence, for the Carrara, Fossacava and Rif. Belvedere rain gauges and for the CMB.

The probabilistic ID thresholds are well-defined in the range of D 3–100 h for Carrara, Fossacava and the CMB, and in the range 2–100 h for Rif. Belvedere (Fig. 8 and Table 6). Inspection of Fig. 8 indicates that for $D = 3$ h, the probabilistic thresholds (probability 10–90%) for Carrara, Fossacava, Rif. Belvedere and the CMB are defined in the range of rainfall intensity (I) 10.8–24.2, 20.8–29.6, 15.1–26.7, and 11.9–26.8 mm h⁻¹, respectively. While for $D = 100$ h, they are defined as 0.6–1.4, 1.0–1.4, 1.2–2.0 and 0.9–2.1 mm h⁻¹, respectively.

The ID thresholds fall into an intensity range wider at Carrara (Fig. 8a) than at Fossacava (Fig. 8b) and Rif. Belvedere (Fig. 8c). This may be due to a greater number of rainfall data (69) and to a misclassifications between DF and NDF events; consequently, the thresholds for Carrara are more conservative than those for Fossacava and Rif. Belvedere. The ID thresholds for the CMB are included in the highest range of rainfall intensity (Fig. 8d). This is due to joining of the rainfall data

recorded at each of 191 rain gauges (Table 2) and the resultant highest number of misclassifications between DF and NDF events (Fig. 8d).

The probabilistic ED thresholds are well-defined in the D range of 3–100 h (Fig. 9 and Table 6). The graphs in Fig. 9 indicate that for $D = 3$ h, the ED thresholds (probability 10–90%) are defined in the range of cumulated rainfall (E) 32.2–73.3, 62.3–88.2, 45.1–80.3, and 35.6–81.1 mm, for Carrara, Fossacava, Rif. Belvedere and the CMB, respectively (Fig. 9). For $D = 100$ h, the thresholds are defined as 59.5–135.5, 99.6–150.0, 115.8–206.3, and 93.5–212.8 mm, respectively (Fig. 9). Likewise for I , the range of the cumulated event rainfall between 10% and 90% probability, ED thresholds are wider for Carrara (Fig. 9a) and the CMB (Fig. 9d) than for Fossacava (Fig. 9b) and Rif. Belvedere (Fig. 9c). This is due to the larger number of overlapping between DF and NDF events for the Carrara rain gauge than for the others.

The high p -values of β_1'' for the Carrara and Fossacava rain gauges (0.127 and 0.254, respectively; Table 4) is related to the slope values of the lines very close to zero (0.18 and 0.13, respectively; Fig. 9a,b and Table 6). This means that the probabilistic ED thresholds for Carrara (Fig. 9a) and Fossacava (Fig. 9b) are almost parallel to the x -axis. Differently, the p -value of β_1'' and the slope values of the ED thresholds for the CMB are the highest. This means that the combination of the rainfall data of all the rain gauges allows us to increase the importance of the rainfall duration to discriminate the rainfall conditions triggering debris flows.

Finally, inspection of the probabilistic $E_{MAP}I$ thresholds (Fig. 10 and Table 6) indicates that E_{MAP} decreases with increasing I . The $E_{MAP}I$ thresholds for Carrara are the most conservative, while those for Fossacava are the highest, and those for the CMB fall between the two. The high p -values of β_1''' for Carrara (0.117) and Fossacava (0.254; Table 5) are related to the slope of the lines very close to zero. The lines showing the $E_{MAP}I$ thresholds for Carrara ($\gamma = 0.22$) and Fossacava ($\gamma = 0.15$) are less steep than those for Rif. Belvedere ($\gamma = 0.37$) and the CMB ($\gamma = 0.33$). This means that for Carrara and Fossacava I is less important than E_{MAP} to discriminate the rainfall conditions triggering debris flows.

7.2. ROC analysis of the logistic regression results

In order to evaluate the results of the logistic regression in defining the probabilistic thresholds, the contingency tables were created, the contingencies and skill scores were computed, and an ROC analysis was performed. Contingencies and skill scores were computed for all the thresholds, but only those derived for the CMB (Tables 7, 8 and 9) are shown here. Tables 7, 8 and 9 show the four contingencies (true positives, false negatives, false positives, and true negatives) and six skill scores (POD , $POFD$, $POFA$, E_f , HK , and δ) for the ID , ED and E_{MAPI} thresholds, at different probability levels (from 10% to 90%). The contingencies and skill scores for the ED and E_{MAPI} thresholds are very similar to those for the ID thresholds; they are shown in Tables 8 and 9 but not discussed here. Table 7 and Fig. 8d indicate that, for the 10% probability ID threshold: two false negatives (red diamonds in Fig. 8d) fall below the threshold, 69 true positives (red diamonds) fall above the threshold, 85 false positives (green squares in Fig. 8d) fall above the threshold, and 35 true negatives (green squares) fall below the threshold. Consequently, the POD , $POFD$, and $POFA$ values are 0.97, 0.71, and 0.55, respectively. Otherwise, for the 90% probability ID threshold (Fig. 8d and Table 7), 57 false negatives (red diamonds in Fig. 8d) fall below the threshold and 14 true positives (red diamonds) fall above the threshold, while no false positives (green squares) fall above the threshold, and 120 true negatives (green squares) fall below the threshold. Hence, the POD , $POFD$ and $POFA$ values are 0.20, 0.00 and 0.00, respectively. Tables 7, 8 and 9 indicate that, for all types of rainfall threshold, the optimal value of POD is obtained for the 10% probability threshold, while the optimal values of $POFD$ and $POFA$ are obtained for the 90% probability threshold. Fig. 11 shows ROC curves and AUC values of the ID , ED and E_{MAPI} thresholds for each rain gauge (Carrara, Fossacava and Rif. Belvedere) and for the CMB. All the AUC values are similar and higher than 0.84. This means that the predictive capability of the three types of threshold is acceptable both for each rain gauge and for the whole study area. In particular, the best predictions

of debris flow occurrence were obtained for the Fossacava rain gauge, as evidenced by its *AUC* values. Each black dot in the graphs of Fig. 11 represents a CMB threshold (*POD* and *POFD* couple) for a different probability of debris flow occurrence. As proposed by Gariano et al. (2015), for each couple of (*POD*, *POFD*) data, the Euclidean distance δ from the perfect classification was calculated (black square in the upper left corner of the ROC spaces; Fig. 11).

Contingencies and skill scores listed in Tables 7, 8 and 9 allow us to choose the optimal probability threshold for each threshold type (*ID*, *ED*, and *E_{MAP}I*). Independently of the threshold type, the highest values of *HK* were obtained for the 40% probability threshold; whereas the highest values of *E_f* were obtained for 40% probability *ID* threshold and for 60% probability *ED* and *E_{MAP}I* thresholds. The smallest distance δ from the perfect classification was also obtained for the 40% probability threshold. The best compromise between the maximum number of correct debris flow predictions (*TP* and *TN*) and the number of wrong predictions (*FP* and *FN*) was calculated for the 40% probability *ID* threshold and for the 60% probability *ED* and *E_{MAP}I* thresholds. The largest difference between correct and incorrect predictions corresponds to the 60% probability *E_{MAP}I* threshold: $(TP + TN) - (FP + FN) = 117$. Moreover, based on the analysis of contingencies and skill scores, the 40% probability threshold can be considered the best performing (*optimal*) for all types of regression from a statistical point of view.

The median of the duration of the DF events for the CMB is 19 h, while 24 h is a typical value used in determining the intensity–duration–frequency curves (Chen, 1983; Kao and Ganguly, 2011) and in defining the return periods of extreme rainfalls (Caporali et al., 2014b). Therefore, the use of these rainfall duration values is considered appropriate to describe the thresholds with the 40% probability of debris flow occurrence. For the 40% probability *ID* threshold, the intensities are 4.6 and 3.7 mm h⁻¹ for rainfall durations of 19 and 24 h, respectively. For the 40% probability *ED* threshold, the cumulative rainfalls are 82.8 and 88.3 mm for rainfall durations of 19 and 24 h, respectively. Finally, the average intensity of the rainfall analyzed for the CMB is 5 mm h⁻¹. For this intensity the *E_{MAP}* value related to 40% probability *E_{MAP}I* threshold is 5.1.

7. Conclusions

Large amounts of quarry waste in the CMB can be involved in slope instability and represent a danger to people and their activities. Quarrying causes morphological changes, making difficult to provide countermeasures for landslide prevention, such as slope re-profiling, retaining walls and check dams. On the other hand, the complete removal of the waste could be counterproductive, because it can mitigate and slow down flooding. Therefore, the knowledge of the minimum rainfall amount inducing debris flows is very helpful.

With this goal, the data recorded from 1950 to 2005 by three rain gauges in the CMB were analyzed and compared with the occurrence of debris flows involving the quarry waste. The three rain gauges have different elevations and operating periods; consequently, the rainfall thresholds were determined for each rain gauge and for the whole study area, based on three couple of rainfall variables: ID , ED , and E_{MAPI} .

The rainfall events were classified into DF and NDF events and, using logistic regression, thresholds of different probability of debris flow occurrence (from 10% to 90%) were determined. Independently of the rainfall variables chosen, the probabilistic thresholds for Carrara are the lowest, while those for Fossacava are the highest, and those for Rif. Belvedere and CMB fall between the two. The goodness of fit of the logistic regression in defining the thresholds was evaluated by means of a ROC analysis. The AUC values for all the thresholds of the CMB are similar and higher than 0.84. This means that the predictive capability of the three types of threshold is acceptable. Moreover, the contingencies and the skill scores indicate that the best compromise between number of correct predictions and the number of incorrect predictions is obtained for the 40% probability threshold for each rain gauge and for the whole CMB, independently of the threshold type.

The probabilistic thresholds obtained for the CMB can provide a guidance to set up debris flow warning systems and plan emergency actions. Decisions on warning and emergency responses can

be based on the comparison of rainfall measurement and forecast with empirical rainfall thresholds. Automated analysis of real-time rainfall and digital quantitative precipitation forecast are needed to fully implement a warning system based on rainfall thresholds (Chleborad et al., 2008). The thresholds can be compared with the measured rainfall amount (variation of the rainfall variable from the beginning of the rainfall event) and/or the forecasted rainfall amount. For example, the evolution of a certain event can be more easily observed and interpreted visualizing the temporal evolution of the cumulative rainfall and overlaying its graphic to the probabilistic *ED* thresholds. The evolution of a rainstorm can be followed in the graph of the probabilistic thresholds; consequently, the increasing probability of debris flow occurrence can be assessed in real time. When the rainfall gets close to or exceeds a prearranged probability threshold, appropriate emergency actions can be adopted for the expected risk scenario. This approach needs to be tested for a certain period, but can help the civil protection authorities in planning emergency actions.

Acknowledgements

We are grateful to the Tuscany Region Hydrologic Service (in particular to Dr. Luca Pisani and Dr. Paolo Del Santo), to the Agro-meteorological Regional Agency (A.R.S.I.A.) for giving us the rainfall data, and to Dr. Stefano Piccioli (geologist) for his contribution in data collection. We also thank the Editor Prof. Takashi Oguchi, Dr. Greg Whitfield and an anonymous reviewer, whose comments and suggestions greatly improved this paper.

References

- Aleotti, P., 2004. A warning system for rainfall-induced shallow failures. *Engineering Geology* 73, 247–265.
- Agresti, A., 2010. *Analysis of ordinal categorical data*, Second Edition. John Wiley & Sons, Inc.

- Baldacci, F., Cecchini, S., Lopane, G., Raggi, G., 1993. Le risorse idriche del Fiume Serchio ed il loro contributo all'alimentazione dei bacini idrografici adiacenti. *Memorie della Società Geologica Italiana* 49, 365–391.
- Barnes, L.R., Schultz, D.M., Grunfest, E.C., Hayden, M.H., Benight, C.C., 2009. CORRIGENDUM: False alarm rate or false alarm ratio?. *Weather Forecast* 24, 1452–1454.
- Baroni, C., Bruschi, G., Ribolini, A., 2000. Human-induced hazardous debris flows in Carrara marble basins (Tuscany, Italy). *Earth Surface Processes and Landforms* 25, 93–103.
- Baroni, C., Bruschi, G., Criscuolo, A., Mandrone, G., 2003. An extensive range grain-size analyses in the source areas of the Carrara marble basins debris flows (Apuane Alps, Italy). In: Rickenmann, D., Chen, C.L. (Eds.), *Debris-Flow Hazard Mitigation: Mechanics, Prediction, and Assessment*. Third International Conference on Debris-Flow Hazards Mitigation. Davos, Switzerland, pp. 809–820.
- Baroni, C., Ribolini, A., Bruschi, G., Mannucci, P., 2010. Geomorphological map and raised-relief model of the Carrara marble basins, Tuscany, Italy. *Geografia Fisica e Dinamica Quaternaria* 33, 233–243.
- Bartelletti, C., D'Amato Avanzi G., Galanti, Y., Giannecchini, R., Mazzali, A., 2015. Assessing shallow landslide susceptibility by using the SHALSTAB model in Eastern Liguria (Italy). *Rendiconti Online Società Geologica Italiana* 35, 17–20.
- Barton, N.R., 2008. Shear strength of rockfill, interfaces and rock joints, and their points of contact in rock dump design. In: Furie, A. (Ed.), *Rock Dumps 2008 Proceedings*. Australian Centre for Geomechanics, Perth, pp. 3–17.
- Barton, N.R., Kjaernsli, B., 1981. Shear strength of rockfill. *Journal of the Geotechnical Engineering Division*, 107 (7), 873–891.

- Baum, R.L., Godt, J.W., 2010. Early warning of rainfall-induced shallow landslides and debris flows in the USA. *Landslides* 7, 259–272.
- Baum, R.L., Godt, J.W., Savage W.Z., 2010. Estimating the timing and location of shallow rainfall-induced landslides using a model for transient, unsaturated infiltration. *Journal of Geophysical Research: Earth Surface* 115, F03013. doi:10.1029/2009JF001321
- Bordoni, M., Meisina, C., Valentino, R., Lu, N., Bittelli, M., Chersich, S., 2015. Hydrological factors affecting rainfall-induced shallow landslides: From the field monitoring to a simplified slope stability analysis. *Engineering Geology* 193, 19–37.
- Brunetti, M.T., Peruccacci, S., Rossi, M., Luciani, S., Valigi, D., Guzzetti, F., 2010. Rainfall thresholds for the possible occurrence of landslides in Italy. *Natural Hazards and Earth System Sciences* 10, 447–458.
- Bruschi, G., Criscuolo, A., Peribeni, E., Zanchetta, G., 2004. ^{14}C -dating from an old quarry waste dump of Carrara marble (Italy): evidence of pre-Roman exploitation. *Journal of Cultural Heritage* 5, 3–6.
- Caine, N., 1980. The rainfall intensity-duration control of shallow landslides and debris flows. *Geografiska Annaler* 62A (1–2), 23–27.
- Calvello, M., d’Orsi, R.N., Piciullo, L., Paes, N., Magalhaes, M., Lacerda, W.A., 2015. The Rio de Janeiro early warning system for rainfall-induced landslides: Analysis of performance for the years 2010–2013. *International Journal of Disaster Risk Reduction* 12, 3–15.
- Cannon, S.H., 1988. Regional rainfall-threshold conditions for abundant debris-flow activity. In: Ellen, S.D., Wiczorek, G.F. (Eds.), *Landslides, floods, and marine effects of the storm of January 3–5, 1982, in the San Francisco Bay Region, California*. U.S. Geological Survey Professional Paper 1434, United States Government Printing Office, Washington, pp. 35–42.

- Cannon, S.H., Ellen, S.D., 1988. Rainfall that resulted in abundant debris flows activity during the storm. In: Ellen, S.D., Wieczorek, G.F. (Eds.), Landslides, floods, and marine effects of the storm of January 3–5, 1982, in the San Francisco Bay Region, California. U.S. Geological Survey Professional Paper 1434, United States Government Printing Office, Washington, pp. 27–33..
- Cannon, S.H., Gartner, J.E., Wilson R.C., Bowers J.C., Laber J.L., 2008. Storm rainfall conditions for floods and debris flows from recently burned areas in southwestern Colorado and southern California. *Geomorphology* 96, 250–269.
- Cannon, S.H., Boldt, E.M., Laber, J.L., Kean, J.W., Staley, D.M., 2011. Rainfall intensity–duration thresholds for postfire debris-flow emergency-response planning. *Natural Hazards* 59, 209–236.
- Caporali, E., Chiarello, V., Rossi G., 2014a. Analisi di frequenza regionale delle precipitazioni estreme. Technical report, University of Florence, Italy. http://www.regione.toscana.it/documents/10180/11615148/Relaz_B1_finale_Marzo2014.pdf/c109e11a-96be-4095-9424-415db468da23.
- Caporali, E., Chiarello, V., Rossi G., 2014b. Regional Frequency Analysis of extreme rainfall events, Tuscany (Italy). *American Geophysical Union*, vol. H41A, pp. 769–769.
- Centro Funzionale Regione Toscana, 2015. Analisi di Frequenza Regionale delle Precipitazioni Estreme - LSPP - Aggiornamento al 2012. <http://www.sir.toscana.it/index.php?IDS=4&IDSS=19>. Accessed 30 July 2015.
- Chang, K-t., Chiang, S-H., Lei, F., 2008. Analysing the relationship between typhoon-triggered landslides and critical rainfall conditions. *Earth Surface Processes and Landforms* 33, 1261–1271.
- Chen, C-l., 1983. Rainfall intensity-duration-frequency formulas. *Journal of Hydraulic Engineering* 109, 1603–1621.
- Chleborad, A. F., Baum, R.L., Godt, J.W., Powers, P.S., 2008. A prototype system for forecasting landslides in the Seattle, Washington, area. *Reviews in Engineering Geology* 20, 103–120.

- Conti, P., Carmignani, L., Giglia, G., Meccheri, M., Fantozzi, P.L., 2004. Evolution of geological interpretations in the Alpi Apuane metamorphic complex, and their relevance for geology of the Northern Apennines. In: Morini, D., Bruni, P. (Eds.), The 'Regione Toscana' project of geological mapping, Spec vol. for the 32nd International Geological Congress, Florence, Italy, pp. 241–262.
- Cortopassi, P.F., Daddi, M., D'Amato Avanzi, G., Giannecchini, R., Lattanzi, G., Merlini, A., Milano, P.F., 2008. Quarry waste and slope instability: preliminary assessment of some controlling factors in the Carrara marble basin (Italy). *Italian Journal of Engineering Geology and Environment*, Special Issue 1, 99–118.
- Cruden, D.M., Varnes, D.J., 1996. Landslide type and processes. In: Turner, A.K., Schuster, R.L. (Eds.), *Landslide: Investigation and Mitigation*, Transportation Research Board, National Academy of Sciences, Special Report 24, Washington, DC, pp. 36–75.
- D'Amato Avanzi, G., Verani, V., 2000. Quarrying activities and geosites of the Apuan Alps (north-western Tuscany, Italy): coexistence possibilities and protection criteria. *Memorie Descrittive della Carta Geologica d'Italia* 54, 121–128.
- D'Amato Avanzi, G., Giannecchini, R., Puccinelli, A., 2004. The influence of the geological and geomorphological settings on shallow landslides. An example in a temperate climate environment: the June 19, 1996 event in northwestern Tuscany (Italy). *Engineering Geology* 73, 215–228.
- D'Amato Avanzi, G., Falaschi, F., Giannecchini, R., Puccinelli, A., 2009. Soil slip susceptibility assessment using mechanical–hydrological approach and GIS techniques: an application in the Apuan Alps (Italy). *Natural Hazards* 50, 591–603.
- D'Amato Avanzi, G., Galanti, Y., Giannecchini, R., 2010. The landslides triggered by the December 2009 meteorological events in North-Western Tuscany (Italy): First results. *Rendiconti Online Società Geologica Italiana* 11 (2), 583–584.

- D'Amato Avanzi, G., Galanti, Y., Giannecchini, R., Puccinelli, A., 2013a. Fragility of territory and infrastructures resulting from rainstorms in Northern Tuscany (Italy). In: Margottini, C., Canuti, P., Sassa, K. (Eds.), *Landslide Science and Practice*. Springer Berlin Heidelberg, Berlin, pp. 239–246.
- D'Amato Avanzi, G., Galanti, Y., Giannecchini, R., Lo Presti, D., Puccinelli, A., 2013b. Estimation of soil properties of shallow landslide source areas by dynamic penetration tests: first outcomes from Northern Tuscany (Italy). *Bulletin of Engineering Geology and the Environment* 72 (3), 609–624.
- Dahal, R.K., Hasegawa, S., 2008. Representative rainfall thresholds for landslides in the Nepal Himalaya. *Geomorphology* 100, 429–443.
- Ellen, S.D., Fleming, R.W., 1987. Mobilization of debris flows from soil slips, San Francisco Bay region, California. *Reviews in Engineering Geology* 7, 31–40.
- Fawcett T., 2006. An introduction to ROC analysis. *Pattern Recognition Letters* 27 (8), 861–874.
- Frattoni, P., Crosta, G., Sosio, R., 2009. Approaches for defining thresholds and return periods for rainfall-triggered shallow landslides. *Hydrological Processes* 23 (10), 1444–1460.
- Gariano, S.L., Brunetti, M.T., Iovine, G., Melillo, M., Peruccacci, S., Terranova, O., Vennari, C., Guzzetti, F., 2015. Calibration and validation of rainfall thresholds for shallow landslide forecasting in Sicily, southern Italy. *Geomorphology* 228, 653–665.
- Giannecchini, R., 2006. Relationship between rainfall and shallow landslides in the southern Apuan Alps (Italy). *Natural Hazards and Earth System Science* 6, 357–364.
- Giannecchini, R., D'Amato Avanzi, G., 2012. Historical research as a tool in estimating hydrogeological hazard in a typical small alpine-like area: The example of the Versilia River basin (Apuan Alps, Italy). *Journal of Physics and Chemistry of the Earth, Parts A/B/C* 49, 32–43.

- Giannecchini, R., Naldini, D., D'Amato Avanzi, G., Puccinelli, A., 2007. Modelling of the initiation of rainfall-induced debris flows in the Cardoso basin (Apuan Alps, Italy). *Quaternary International* 171–172, 108–117.
- Giannecchini, R., Galanti, Y., D'Amato Avanzi, G., 2012. Critical rainfall thresholds for triggering shallow landslides in the Serchio River Valley (Tuscany, Italy). *Natural Hazards and Earth System Science* 12, 829–842.
- Giannecchini, R., Galanti, Y., Barsanti, M., 2015. Rainfall intensity-duration thresholds for triggering shallow landslides in the Eastern Ligurian Riviera (Italy). In: Lollino, G., Giordan, D., Crosta, G.B., Corominas, J., Azzam, R., Wasowski, J., Sciarra, N. (Eds.), *Engineering Geology for Society and Territory – Volume 2*. Springer International Publishing, Switzerland, pp. 1581–1584.
- Godt, J.W., Baum, R.L., Chleborad, A.F., 2006. Rainfall characteristics for shallow landsliding in Seattle, Washington, USA. *Earth Surfaces Processes and Landforms* 31 (1), 97–110.
- Guidicini, G., Iwasa, O.Y., 1977. Tentative correlation between rainfall and landslides in a humid tropical environment. *Bulletin International Association Engineering Geology* 16 (1), 13–20.
- Guzzetti, F., 2000. Landslide fatalities and the evaluation of landslide risk in Italy. *Engineering Geology* 58 (2), 89–107.
- Guzzetti, F., Stark, C.P., Salvati, P., 2005. Evaluation of flood and landslide risk to the population of Italy. *Environmental Management* 36 (1), 15–36.
- Guzzetti, F., Peruccacci, S., Rossi, M., Stark, C.P., 2007. Rainfall thresholds for the initiation of landslides in central and southern Europe. *Meteorology and Atmospheric Physics* 98 (3), 239–267.
- Guzzetti, F., Peruccacci, S., Rossi, M., Stark, C.P., 2008. The rainfall intensity-duration control of shallow landslides and debris flows: an update. *Landslides* 5 (1), 3–17.

- Hanssen, A.W., Kuipers, W.J.A., 1965. On the relationship between the frequency of rain and various meteorological parameters. 81. Koninklijk Nederlands Meteorologisch Instituut, Meded. Verhand, pp. 2–15.
- Hungr, O., Evans, S.G., Bovis, M.J., Hutchinson, J.N., 2001. A review of the classification of landslides of the flow type. *Environmental & Engineering Geoscience* 7 (3), 221–238.
- Hungr, O., Leroueil, S., Picarelli, L., 2014. The Varnes classification of landslide types, an update. *Landslides* 11, 167–194.
- Iverson, R.M., 2000. Landslide triggering by rain infiltration. *Water Resources Research* 36 (7), 1897–1910.
- Iverson, R.M., Reid, M.E., Lahusen, R.G., 1997. Debris-flow mobilization from landslides. *Annual Review in Earth and Planetary Sciences* 25, 85–138.
- Jakob, M., Weatherly, H., 2003. A hydroclimatic threshold for landslide initiation on the North Shore Mountains of Vancouver, British Columbia. *Geomorphology* 54 (3–4), 137–156.
- Kao, S-C., Ganguly, A.R., 2011. Intensity, duration, and frequency of precipitation extremes under 21st-century warming scenarios 116 (D16119), doi:10.1029/2010JD015529.
- Larsen, M.C., Simon, A., 1993. A rainfall intensity-duration threshold for landslides in a humid-tropical environment, Puerto Rico. *Geografiska Annaler* 75A (1–2), 13–23.
- Ma, T., Li, C., Lu, Z., Wang, B., 2014. An effective antecedent precipitation model derived from the power-law relationship between landslide occurrence and rainfall level. *Geomorphology* 216, 187–192.
- Marachi, N.D., Chan, C.K., Seed, H.B., 1972. Evaluation of properties of rockfill materials. *Journal of the Soil Mechanics and Foundations Division* 98 (1), 95–114.

- Martelloni, G., Segoni, S., Fanti, R., Catani, F., 2012. Rainfall thresholds for the forecasting of landslide occurrence at regional scale. *Landslides* 9, 485–495.
- Mathew, J., Babu, D.G., Kundu, S., Kumar, K.V., Pant, C.C., 2014. Integrating intensity–duration–based rainfall threshold and antecedent rainfall-based probability estimate towards generating early warning for rainfall-induced landslides in parts of the Garhwal Himalaya, India. *Landslides* 11 (4), 575–588.
- Melillo, M., Brunetti, M.T., Peruccacci, S., Gariano, S.L, Guzzetti, F., 2015. An algorithm for the objective reconstruction of rainfall events responsible for landslides. *Landslides* 12 (2), 311–320.
- Menard, S.W., 2001. Applied logistic regression analysis, Second Edition. Sage university papers series on Quantitative Applications in the Social Sciences 07-106. Sage Publication Inc. Thousand Oaks, CA.
- Montgomery, D.R., Dietrich, W.E., 1994. A physically based model for the topographic control on shallow landsliding. *Water Resources Research* 30 (4), 1153–1171.
- Panei, G., Forlani, E., Tardi, A., 2000. Sulla stabilità delle discariche di materiali lapidei. *Quarry and Construction* 12, 25–31.
- Peruccacci, S., Brunetti, M.T., Luciani, S., Vennari, C., Guzzetti, F., 2012. Lithological and seasonal control on rainfall thresholds for the possible initiation of landslides in central Italy. *Geomorphology* 139–140, 79–90.
- R Core Team, 2014. R: A Language and Environment for Statistical Computing. R Foundation for Statistical Computing, Vienna. <http://www.R-project.org/>.
- Rianna, G., Pagano, L., Urciuoli, G., 2014. Rainfall patterns triggering shallow flowslides in pyroclastic soils. *Engineering Geology* 174, 22–35.
- Rosi, A., Lagomarsino, D., Rossi, G., Segoni, S., Battistini, A., Casagli, N., 2015. Updating EWS rainfall thresholds for the triggering of landslides. *Natural Hazards* 78 (1), 297–308.

- Rossi, M., Peruccacci, S., Brunetti, M.T., Marchesini, I., Luciani, S., Ardizzone, F., Balducci, V., Bianchi, C., Cardinali, M., Fiorucci, F., Mondini, A.C., Reichenbach, P., Salvati, P., Santangelo, M., Bartolini, D., Gariano, S.L., Palladino, M., Vessia, G., Viero, A., Antronico, L., Borselli, L., Deganutti, A.M., Iovine, G., Luino, F., Parise, M., Polemio, M., Guzzetti, F., Tonelli, G., 2012. SANF: National warning system for rainfall-induced landslides in Italy. In: Eberhardt, E., Froese, C., Turner, K., Leroueil, S. (Eds.), *Landslides and Engineered Slopes: Protecting Society through Improved Understanding*. Taylor & Francis Group, London, pp. 1895–1899.
- Saito, H., Nakayama, D., Matsuyama, H., 2010. Relationship between the initiation of a shallow landslide and rainfall intensity–duration thresholds in Japan. *Geomorphology* 118 (1–2), 167–175.
- Segoni, S., Rosi, A., Rossi, G., Catani, F., Casagli, N., 2014a. Analysing the relationship between rainfalls and landslides to define a mosaic of triggering thresholds for regional-scale warning systems. *Natural Hazards and Earth System Sciences* 14, 2637–2648.
- Segoni, S., Rossi, G., Rosi, A., Catani, F., 2014b. Landslides triggered by rainfall: A semi-automated procedure to define consistent intensity–duration thresholds. *Computers & Geosciences* 63, 123–131.
- Segoni, S., Battistini, A., Rossi, G., Rosi, A., Lagomarsino, D., Catani, F., Moretti, S., Casagli, N., 2015. Technical Note: An operational landslide early warning system at regional scale based on space–time-variable rainfall thresholds. *Natural Hazards and Earth System Sciences* 15, 853–861.
- Staley, D.M., Kean, J.W., Cannon, S.H., Schmidt, K.M., Laber, J.L., 2013. Objective definition of rainfall intensity–duration thresholds for the initiation of post-fire debris flows in southern California. *Landslides* 10 (5), 547–562.
- Swets, J. A., 1988. Measuring the accuracy of diagnostic systems. *Science* 240 (4857), 1285–1293.
- Terlien, M.T.J., 1998. The determination of statistical and deterministic hydrological landslide-triggering thresholds. *Environmental Geology*, 35 (2), 124–130.

- Tien Bui, D., Pradhan, B., Lofman, O., Revhaug, I., Dick, Ø.B., 2013. Regional prediction of landslide hazard using probability analysis of intense rainfall in the Hoa Binh province, Vietnam. *Natural Hazards* 66 (2), 707–730.
- Vennari, C., Gariano, S.L., Antronico, L., Brunetti, M.T., Iovine, G., Peruccacci, S., Terranova, O., Guzzetti, F., 2014. Rainfall thresholds for shallow landslide occurrence in Calabria, southern Italy. *Natural Hazards and Earth System Science* 14, 317–330.
- Wieczorek, G.F., Sarmiento, J., 1988. Rainfall, piezometric level, and debris flows near La Honda, California, in storms between 1975 and 1983. In: Ellen, S.D., Wieczorek, G.F. (Eds.), *Landslides, floods, and marine effects of the storm of January 3–5, 1982, in the San Francisco Bay Region, California*. U.S. Geological Survey Professional Paper 1434, United States Government Printing Office, Washington, pp. 43–62.
- Wu, W., Sidle, R.C., 1995. A distributed slope stability model for steep forested basins. *Water Resources Research* 31 (8), 2097–2110.
- Zêzere, J.L., Vaz, T., Pereira, S., Oliveira, S.C., Marques, R., Garcia, R.A.C., 2015. Rainfall thresholds for landslide activity in Portugal: a state of the art. *Environmental Earth Sciences* 73 (6), 2917–2936.
- Zizioli, D., Meisina, C., Valentino, R., Montrasio, L., 2013. Comparison between different approaches to modeling shallow landslide susceptibility: a case history in Oltrepo Pavese, Northern Italy. *Natural Hazards and Earth System Sciences* 13, 559–573.

Figure Caption List

Fig. 1. The Apuan Alps close to Carrara. Quarries and quarry waste stand out as white areas.

Fig. 2. The Carrara Marble Basin: white areas evidence quarries and quarry waste (base map by Google Earth, captured in 2014).

Fig. 3. Rainfall map of the mean annual precipitation of the Apuan Alps (modified after Baldacci et al., 1993). The box indicates the CMB.

Fig. 4. Active quarry waste mobilized by the 23 September 2003 heavy rainstorm in the CMB. (a) Waste material occupying a valley bottom; (b) scars and tracks on a large quarry dump; (c) large fan of debris flow; and (d) debris flow with the source area, track and levees.

Fig. 5. Quarry waste involved in landslides (a) and detail of a debris flow track (b), showing the complex texture of a recent quarry deposit (after Cortopassi et al., 2008).

Fig. 6. (a) Contingency table showing the four possible outcomes of a binary classifier model and the five skill scores (POD , $POFD$, $POFA$, Ef , and HK) that can help in the selection of the best threshold. TP : number of true positives; TN : number of true negatives; FP : number of false positives; FN : number of false negatives. (b) ROC space, with three hypothetical ROC curves. $AUC = 0.50$: model with no prediction capabilities. $AUC = 0.79$: model with an acceptable capability of prediction. $AUC = 1$: model with the maximum capability of prediction.

Fig. 7. Seasonal distribution of the main rainstorms recorded at Carrara, Fossacava, Rif. Belvedere and in the whole study area (CMB) from 1950 to 2005. (a) Distribution of all the analyzed rainstorms; (b) distribution of the rainstorms inducing debris flows.

Fig. 8. Probabilistic ID thresholds for (a) Carrara, (b) Fossacava, (c) Rif. Belvedere and (d) CMB. The thresholds at 10%, 30%, 50%, 70% and 90% probability of debris flow occurrence and the related equations are shown.

Fig. 9. Probabilistic ED thresholds for (a) Carrara, (b) Fossacava, (c) Rif. Belvedere and (d) CMB. The thresholds at 10%, 30%, 50%, 70% and 90% probability of debris flow occurrence and the related equations are shown.

Fig. 10. Probabilistic $E_{MAP}I$ thresholds for (a) Carrara, (b) Fossacava, (c) Rif. Belvedere and (d) CMB. The thresholds at 10%, 30%, 50%, 70% and 90% probability of debris flow occurrence and the related equations are shown.

Fig. 11. ROC curve of the ID (a), ED (b) and $E_{MAP}I$ (c) thresholds for each rain gauge and for the CMB. Each $POFD$ – POD couple (black dot) corresponds to a threshold with a specified probability. The perfect classification points (black square in the upper left corner) are also shown. The AUC values for each type of regression are listed. Black lines: Carrara; black dotted lines: Fossacava; gray dotted lines: Rif. Belvedere; gray lines: CMB.

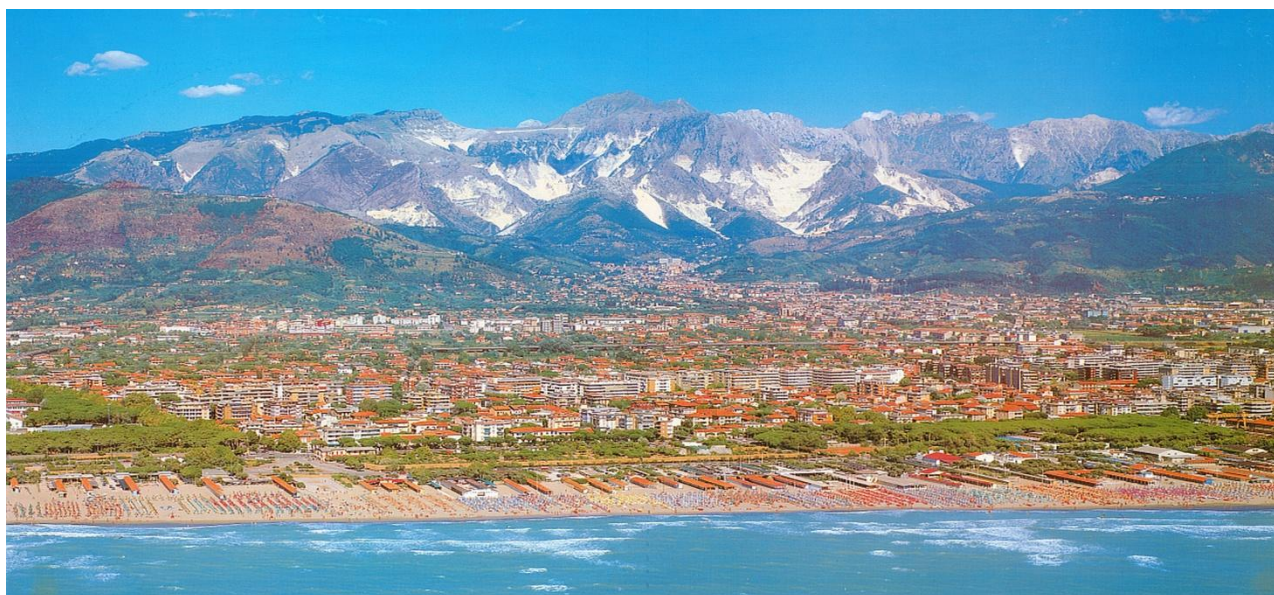


Fig. 1

ACCEPTED MANUSCRIPT

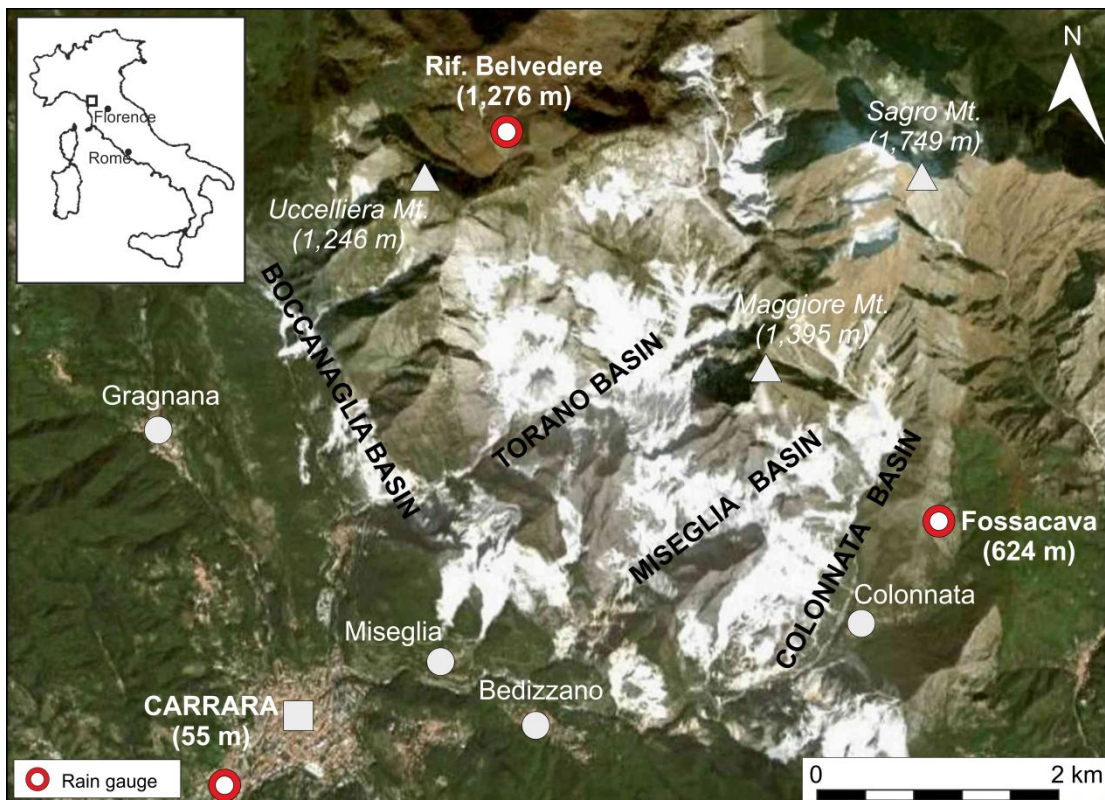


Fig. 2

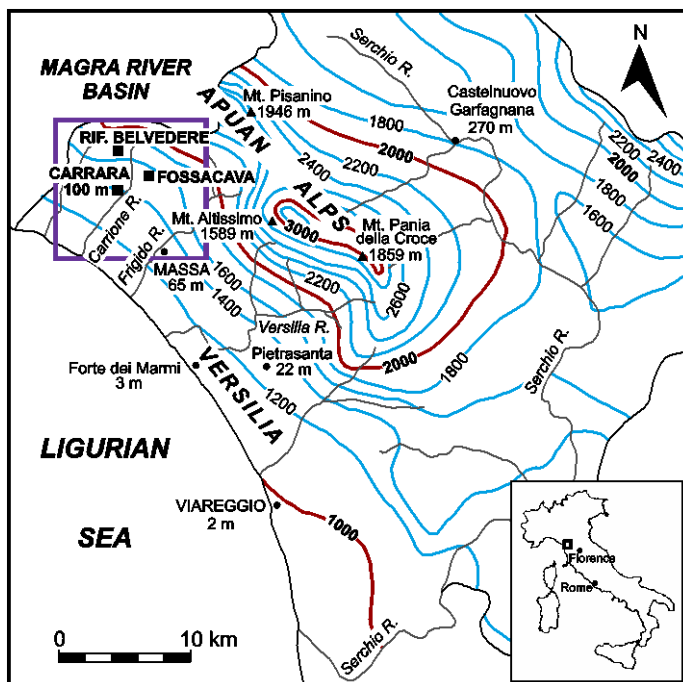


Fig. 3

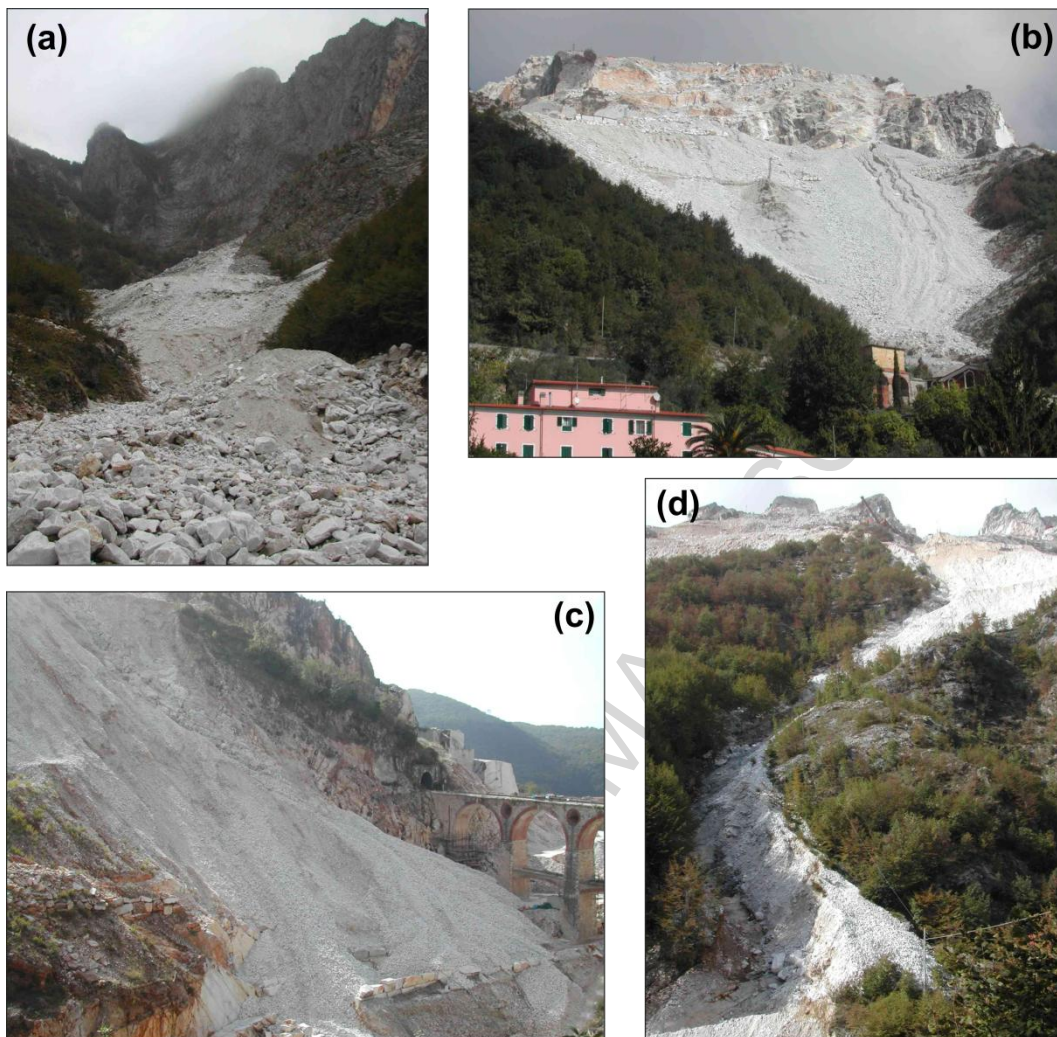


Fig. 4

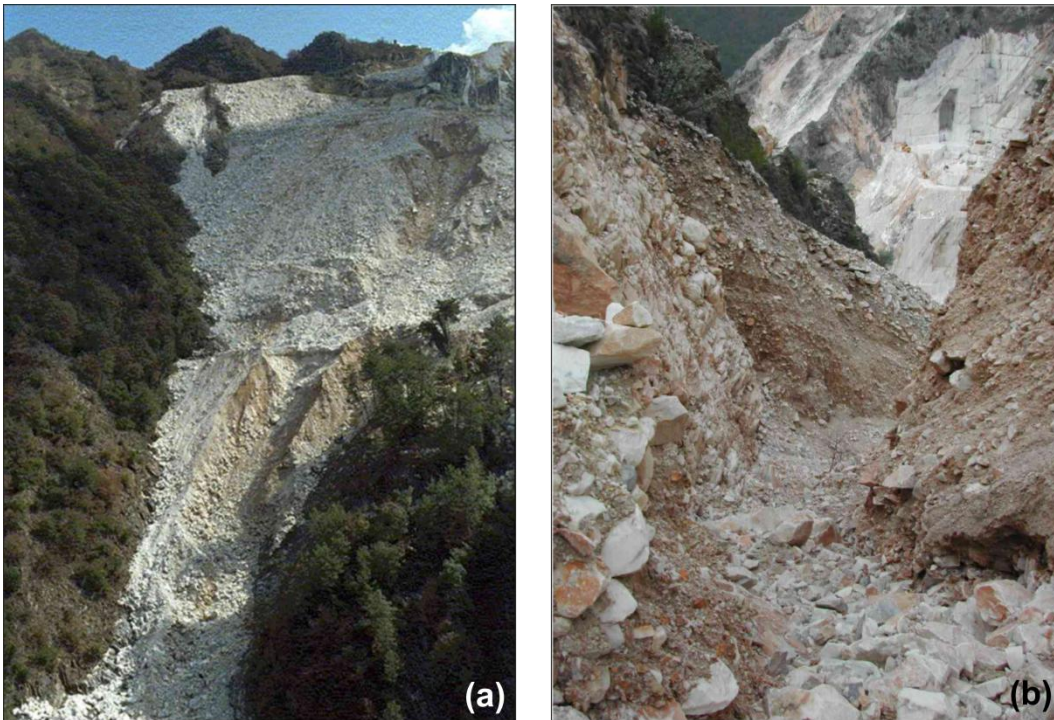


Fig. 5

ACCEPTED MANUSCRIPT

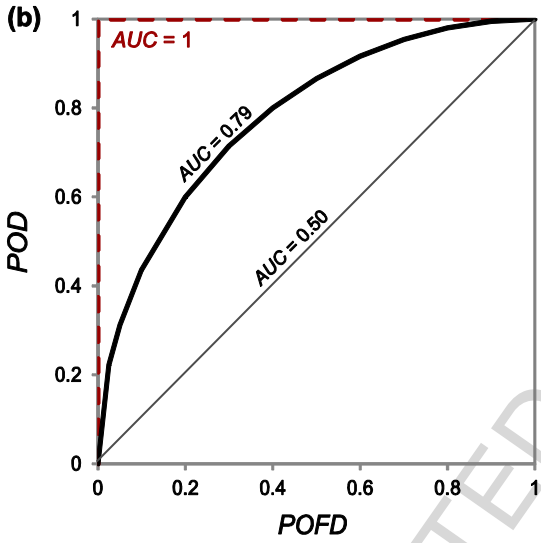
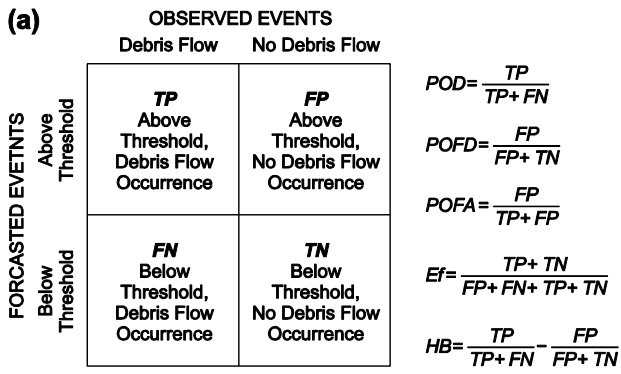


Fig. 6

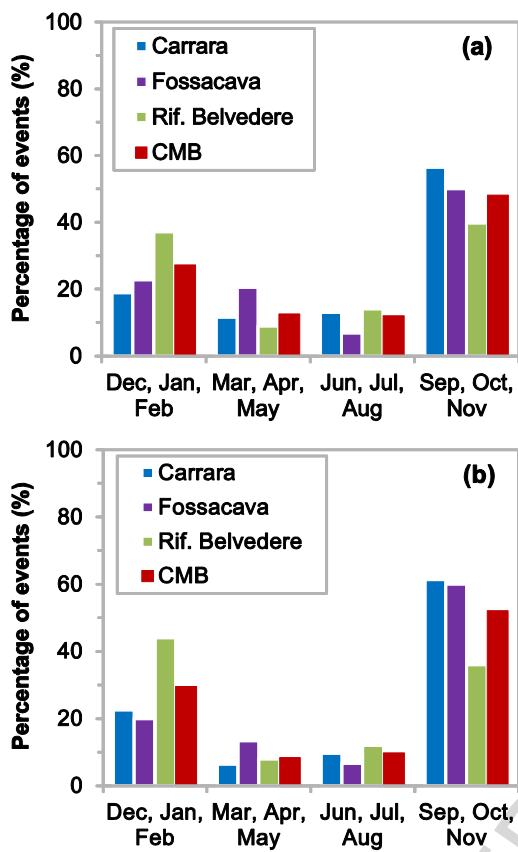


Fig. 7

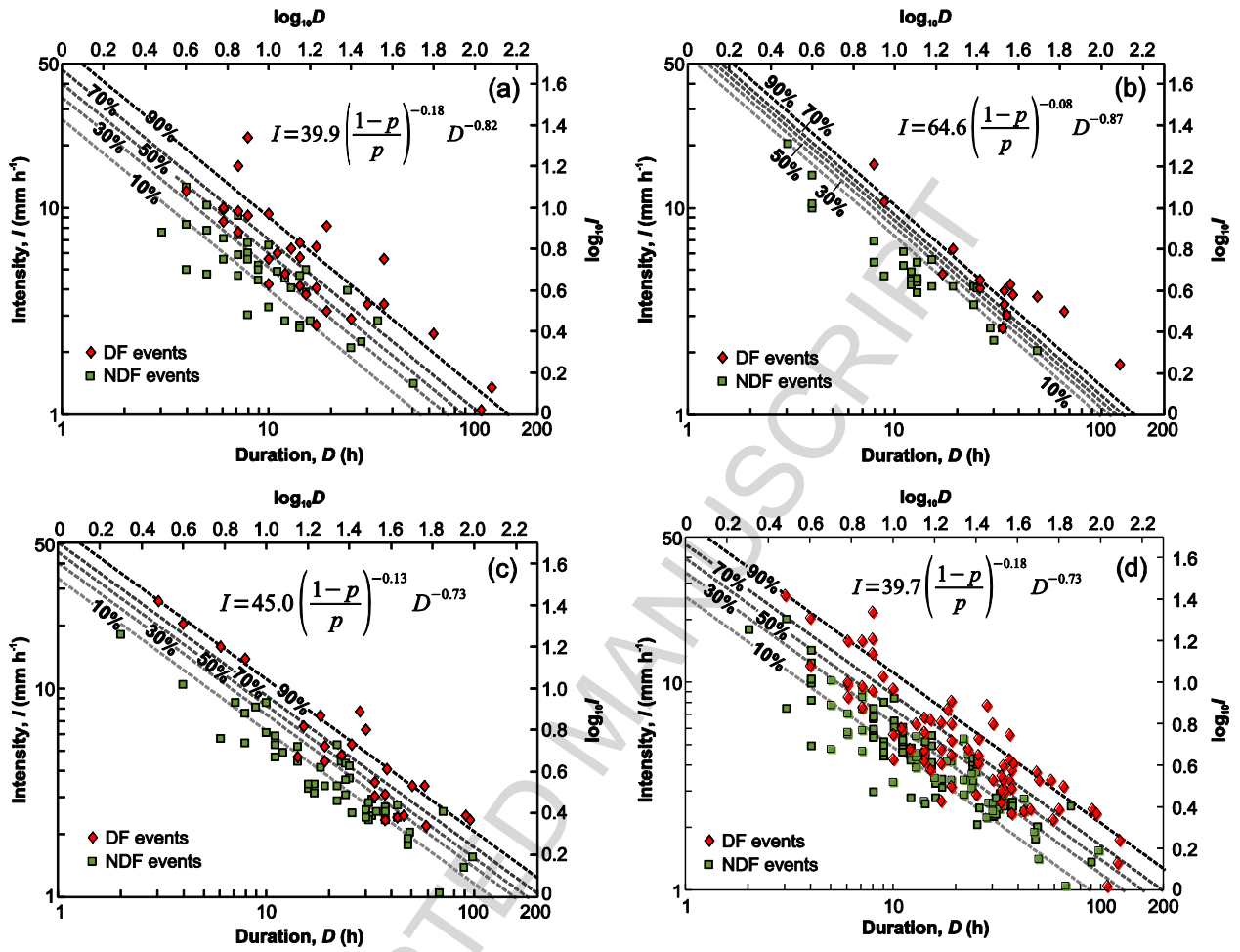


Fig. 8

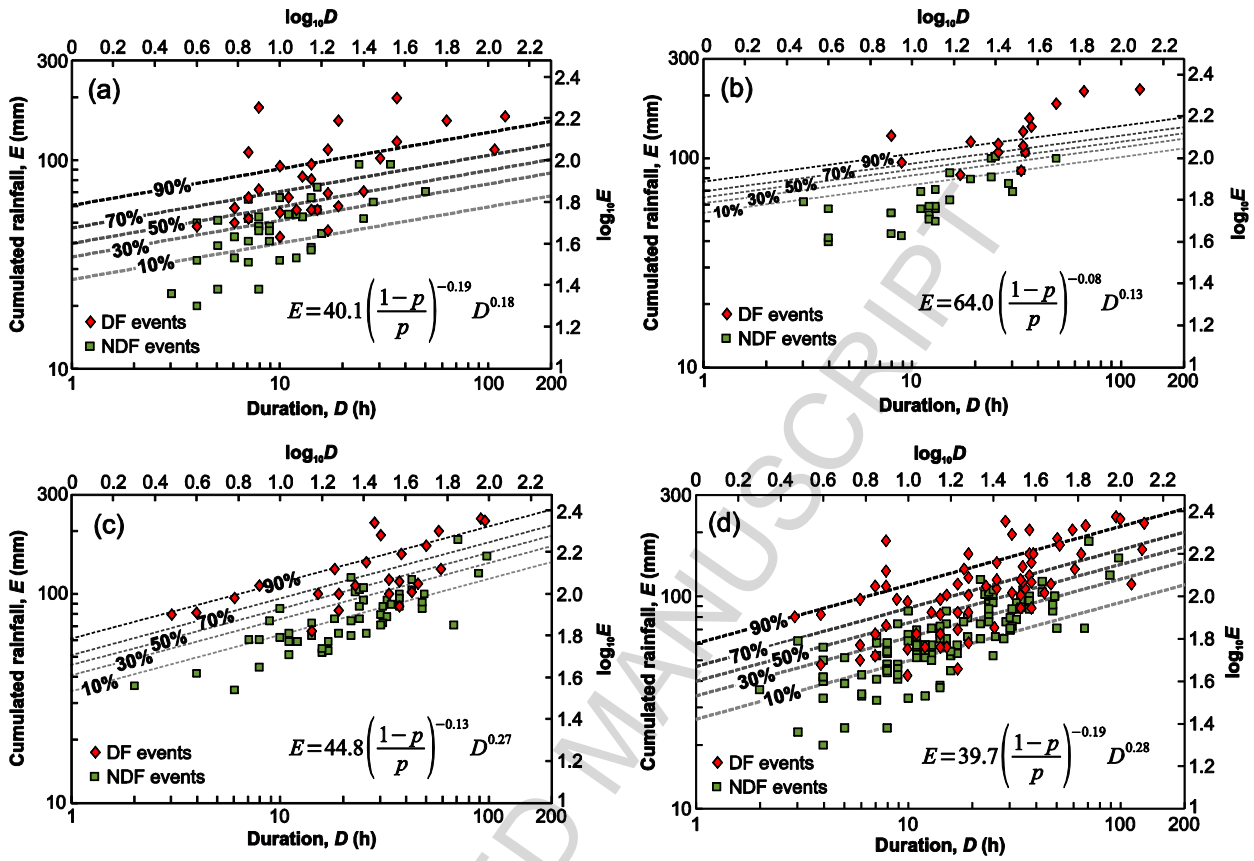


Fig. 9

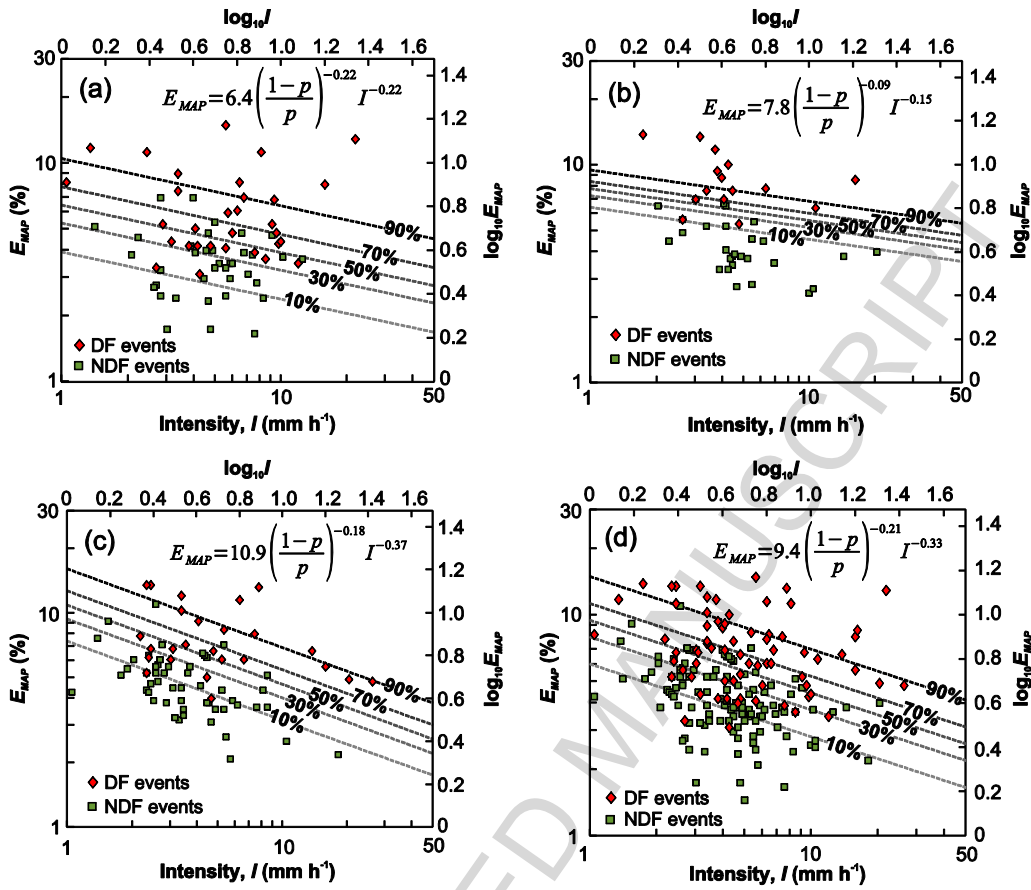


Fig. 10

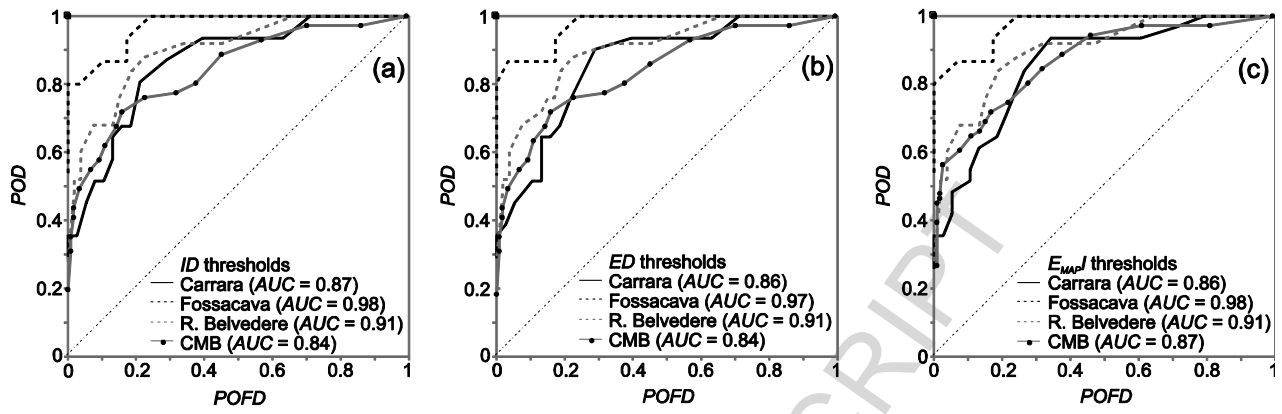


Fig. 11

Table 1. Main rainfall events recorded in Apuan Alps from 1980.

Rainfall event date	Deaths	Source
8 June 1984	2	Giannecchini (2006)
11 July 1992 and 22 August 1992	3	Giannecchini and D'Amato Avanzi (2012)
19 June 1996	14	D'Amato Avanzi et al. (2004)
5 October 1998	-	Giannecchini and D'Amato Avanzi (2012)
6 November 2000	-	Giannecchini (2006)
23 September 2003	1	Cortopassi et al. (2008)
22–23 and 24–25 December 2009	-	D'Amato Avanzi et al. (2010)
31 October 2010	3	D'Amato Avanzi et al. (2013a)
10–11 November 2012	-	Tuscany Region Hydrologic Service
5 November 2014	-	Tuscany Region Hydrologic Service

Table 2. Number and percentage (%) of DF (debris flow) and NDF (no debris flow) recorded in each rain gauge and in all the rain gauges of the CMB.

Rain gauges	DF		NDF		(DF + NDF)
	no.	%	no.	%	no.
Carrara	31	44.9	38	55.1	69
Fossacava	15	35.6	29	64.4	44
Rif. Belvedere	25	32.0	53	68.0	78
CMB	71	37.5	120	62.5	191

Table 3. Best-fit parameters (β_0 , β_1 and β_2) and related p -values for the variables $D-I$ for each rain gauge and for all the rain gauges (CMB).

Rain gauge	Parameter			p -value		
	β_0	β_1	β_2	$p(\beta_0)$	$p(\beta_1)$	$p(\beta_2)$
Carrara	-20.09	4.49	5.45	1.01×10^{-4}	1.23×10^{-4}	2.19×10^{-4}
Fossacava	-51.52	10.77	12.36	3.55×10^{-3}	3.52×10^{-3}	5.11×10^{-3}
Rif. Belvedere	-29.50	5.68	7.75	8.79×10^{-6}	2.62×10^{-5}	8.45×10^{-6}
CMB	-20.00	3.94	5.43	2.59×10^{-11}	9.41×10^{-11}	2.93×10^{-10}

Table 4. Best-fit parameters (β_0'' , β_1'' and β_2'') and related p -values for the variables $D-E$ for each rain gauge and for the CMB.

Rain gauge	Parameter			p -value		
	β_0''	β_1''	β_2''	$p(\beta_0'')$	$p(\beta_1'')$	$p(\beta_2'')$
Carrara	-19.72	-0.94	5.34	1.17×10^{-4}	1.27×10^{-1}	2.59×10^{-4}
Fossacava	-52.61	-1.69	12.65	3.47×10^{-3}	2.20×10^{-1}	5.00×10^{-3}
Rif. Belvedere	-28.92	-2.05	7.61	8.22×10^{-6}	1.87×10^{-3}	7.96×10^{-6}
CMB	-19.67	-1.47	5.34	2.43×10^{-11}	1.06×10^{-4}	2.96×10^{-10}

Table 5. Best-fit parameters (β_0''' , β_1''' and β_2''') and related p -values for the variables $I-E_{MAP}$ for each rain gauge and for the CMB.

Rain gauge	Parameter			p -value		
	β_0'''	β_1'''	β_2'''	$p(\beta_0''')$	$p(\beta_1''')$	$p(\beta_2''')$
Carrara	-8.28	0.96	4.46	2.21×10^{-4}	1.17×10^{-1}	1.34×10^{-4}
Fossacava	-22.39	1.58	10.92	4.07×10^{-3}	2.54×10^{-1}	3.36×10^{-3}
Rif. Belvedere	-13.42	2.07	5.62	3.41×10^{-6}	1.82×10^{-3}	2.52×10^{-5}
CMB	-10.83	1.59	4.82	5.96×10^{-12}	5.56×10^{-5}	2.06×10^{-11}

Table 6. Rainfall thresholds for triggering debris flows for Carrara, Fossacava, Rif. Belvedere and CMB. Type: type of threshold. Equation: D , rainfall duration in hours; I , rainfall intensity in mm h^{-1} ; E , cumulated event rainfall in mm ; E_{MAP} , cumulated event rainfall normalized by MAP . Range: range of validity for the threshold in hours.

Type	Rain gauge	Equation	Range
ID	Carrara	$I = 39.9 \left(\frac{1-p}{p}\right)^{-0.18} D^{-0.82}$	$3 \leq D \leq 100$
	Fossacava	$I = 64.6 \left(\frac{1-p}{p}\right)^{-0.08} D^{-0.87}$	$3 \leq D \leq 100$
	Rif. Belvedere	$I = 45.0 \left(\frac{1-p}{p}\right)^{-0.13} D^{-0.73}$	$2 \leq D \leq 100$
	CMB	$I = 39.7 \left(\frac{1-p}{p}\right)^{-0.18} D^{-0.73}$	$2 \leq D \leq 100$
ED	Carrara	$E = 40.1 \left(\frac{1-p}{p}\right)^{-0.19} D^{0.18}$	$3 \leq D \leq 100$
	Fossacava	$E = 64.0 \left(\frac{1-p}{p}\right)^{-0.08} D^{0.13}$	$3 \leq D \leq 100$
	Rif. Belvedere	$E = 44.8 \left(\frac{1-p}{p}\right)^{-0.13} D^{0.27}$	$2 \leq D \leq 100$
	CMB	$E = 39.7 \left(\frac{1-p}{p}\right)^{-0.19} D^{0.27}$	$2 \leq D \leq 100$
$E_{MAP}I$	Carrara	$E_{MAP} = 6.4 \left(\frac{1-p}{p}\right)^{-0.22} I^{-0.22}$	$1 \leq I \leq 25$
	Fossacava	$E_{MAP} = 7.8 \left(\frac{1-p}{p}\right)^{-0.09} I^{-0.15}$	$1 \leq I \leq 20$
	Rif. Belvedere	$E_{MAP} = 10.9 \left(\frac{1-p}{p}\right)^{-0.18} I^{-0.37}$	$1 \leq I \leq 30$
	CMB	$E_{MAP} = 9.4 \left(\frac{1-p}{p}\right)^{-0.21} I^{-0.33}$	$1 \leq I \leq 30$

Table 7. Contingencies (TP , FP , FN , and TN) and skill scores (POD , $POFD$, $POFA$, Ef , HK , and δ) computed for the ID thresholds of the CMB at different probabilities of debris flow occurrence; best scores are shown in bold. The parameter δ is described in follow.

Probability	TP	FN	FP	TN	POD	$POFD$	$POFA$	Ef	HK	δ
90%	14	57	0	120	0.20	0.00	0.00	0.70	0.20	0.80
80%	26	45	1	119	0.37	0.01	0.04	0.76	0.36	0.63
70%	32	39	2	118	0.45	0.02	0.06	0.79	0.43	0.55
60%	39	32	8	112	0.55	0.07	0.17	0.79	0.48	0.46
50%	44	27	14	106	0.62	0.12	0.24	0.79	0.50	0.40
40%	51	20	19	101	0.72	0.16	0.27	0.80	0.56	0.32
30%	55	16	39	81	0.77	0.33	0.41	0.71	0.45	0.40
20%	63	8	54	66	0.89	0.45	0.46	0.68	0.44	0.46
10%	69	2	85	35	0.97	0.71	0.55	0.54	0.26	0.71

Table 8. Contingencies (TP , FP , FN , and TN) and skill scores (POD , $POFD$, $POFA$, Ef , HK , and δ) computed for the ED thresholds of the CMB at different probabilities of debris flow occurrence; best scores are shown in bold.

Probability	TP	FN	FP	TN	POD	$POFD$	$POFA$	Ef	HK	δ
90%	13	58	0	120	0.18	0.00	0.00	0.70	0.18	0.82
80%	25	46	1	119	0.35	0.01	0.04	0.75	0.34	0.65
70%	31	40	2	118	0.44	0.02	0.06	0.78	0.42	0.56
60%	40	31	8	112	0.56	0.07	0.17	0.80	0.50	0.44
50%	45	26	15	105	0.63	0.13	0.25	0.79	0.51	0.39
40%	51	20	20	100	0.72	0.17	0.28	0.79	0.55	0.33
30%	55	16	39	81	0.77	0.33	0.41	0.71	0.45	0.40
20%	61	10	53	67	0.86	0.44	0.46	0.67	0.42	0.46
10%	69	2	88	32	0.97	0.73	0.56	0.53	0.24	0.73

Table 9. Contingencies (TP , FP , FN , and TN) and skill scores (POD , $POFD$, $POFA$, Ef , HK , and δ) computed for the E_{MAP} thresholds of the CMB at different probabilities of debris flow occurrence; best scores are shown in bold.

Probability	TP	FN	FP	TN	POD	$POFD$	$POFA$	Ef	HK	δ
90%	19	52	1	119	0.27	0.01	0.05	0.72	0.26	0.73
80%	32	39	1	119	0.45	0.01	0.03	0.79	0.44	0.55
70%	34	37	2	118	0.48	0.02	0.06	0.80	0.46	0.52
60%	43	28	9	111	0.61	0.08	0.17	0.81	0.53	0.40
50%	47	24	16	104	0.66	0.13	0.25	0.79	0.53	0.36
40%	51	20	20	100	0.72	0.17	0.28	0.79	0.55	0.33
30%	57	14	33	87	0.80	0.28	0.37	0.75	0.53	0.34
20%	63	8	45	75	0.89	0.38	0.42	0.72	0.51	0.39
10%	69	2	73	47	0.97	0.61	0.51	0.61	0.36	0.61

Highlights

Analysis of 191 rainstorms in a human-modified landscape in 1950-2005 period.

Determination of debris flow probability using logistic regression.

Rainfall thresholds definition for different probability of debris flows occurrence.

Evaluation of thresholds using contingency table, skill scores and ROC analysis.

Proposal of a possible use of rainfall thresholds in debris flow forecasting.

ACCEPTED MANUSCRIPT